2E, arrow). No cells were double-positive for GFP and a neural lineage marker in the injured spinal cord in both the SCI+PBS and SCI+G-CSF groups 24 h after injury (not shown).

To confirm G-CSF-mediated mobilization of bone marrow-derived hematopoietic stem cells, we performed immunohistochemistry for CD34 one week after injury. In the SCI+G-CSF group, GFP- and CD34-double-positive cells were detected near the lesion epicenter (Figs. 2G–I, arrow).

Six weeks after injury, there were many GFP-positive round cells in the lesioned site and cells with some processes in the white matter (Figs. 3A, B). The number of GFP-positive cells in the SCI+G-CSF group was significantly larger than that in the SCI+PBS group 6 weeks after injury (449.0±28.5 in the SCI+PBS group and 610.3±21.9 in the SCI+G-CSF group, $p<0.003$, Fig. 3C). Most of the GFP-positive round cells in the lesioned site were positive for Mac-1, a marker for activated microglia/macrophages (Figs. 4A–C). The number of cells double-positive for GFP and Mac-1 was larger in the SCI+G-CSF group (392.6±44.0; Fig. 5A, hatched column) than that in the SCI+PBS group (338.6±36.4; Fig. 5A, open column). In the white matter, some of the GFP-positive cells were also positive APC (Figs. 4D–F, arrow), whereas there were no GFP- and nestin-double-

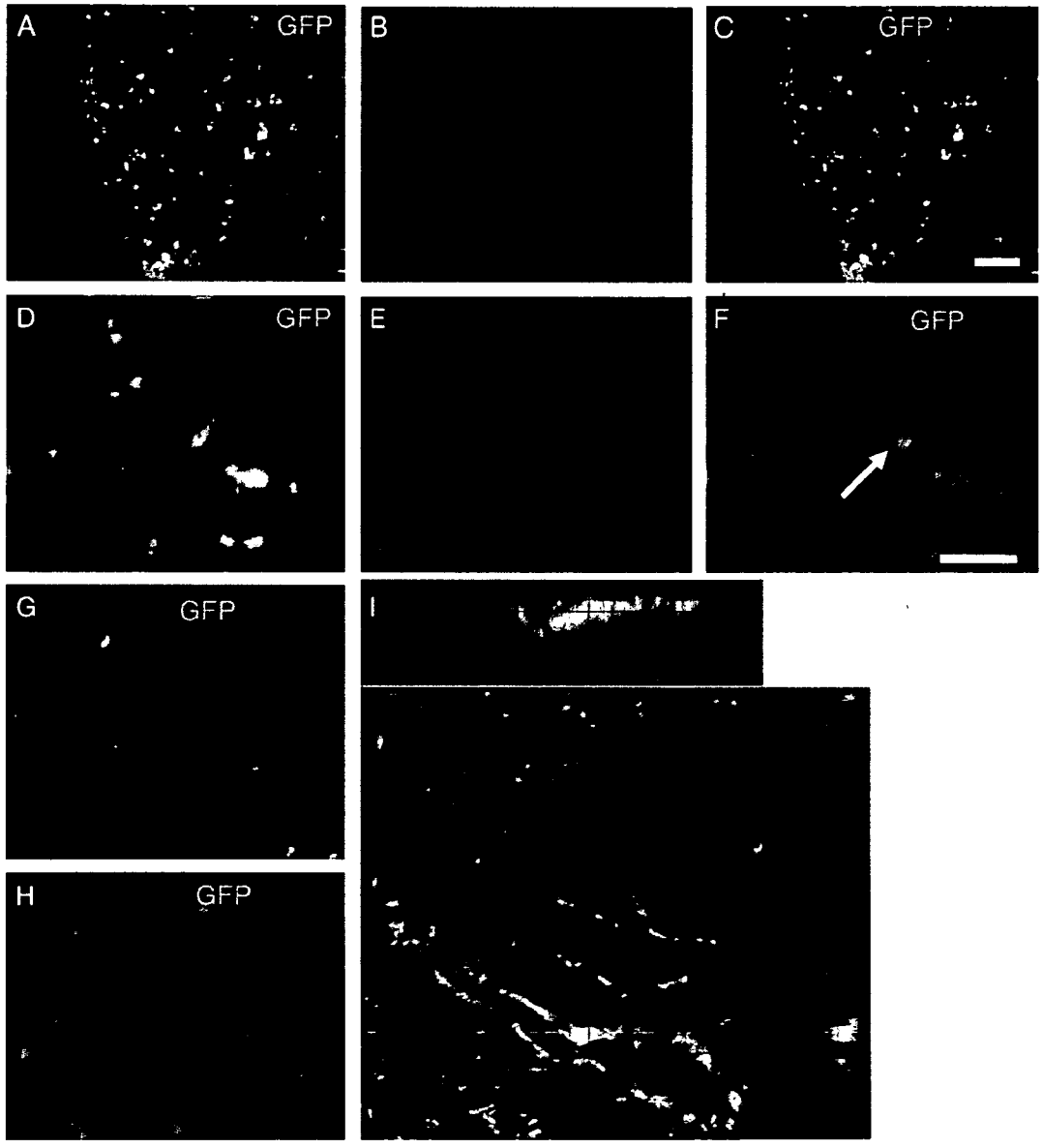

Fig. 4 – Double-immunofluorescence study for GFP and cell-specific markers in the SCI+G-CSF group 6 weeks after injury. Double-positive cells for GFP and Mac-1 (marker for macrophages/microglia; A–C), GFP and GFAP (marker for astrocytes; D–F, arrow), GFP and APC (marker for oligodendrocytes; D–F, arrow), whereas no GFP- and Neu-N (marker for neurons; G) or GFP- and CD-31 (marker for endothelial cells; H)-double-positive cells were observed. Three-dimensional reconstruction of confocal image of double immunofluorescent staining for GFP and GFAP revealed co-localization of GFP and GFAP (I). Bars = 100 μm (A–C) and 50 μm (D–R).

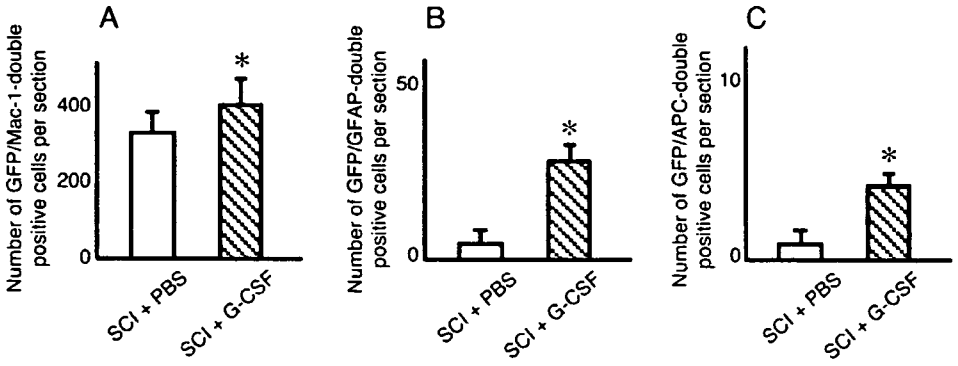

Fig. 5 – Quantitative analysis of double-positive cells for GFP and cell-specific markers 6 weeks after injury. The numbers of double-positive cells for GFP and Mac-1 (A), GFP and GFAP (B), GFP and APC (C) and GFP and nestin (D) were significantly larger in the SCI+G-CSG group than that in the SCI+PBS group. Values are mean±S.E.M. *$p<0.05$.

positive cells (not shown), GFP- and Neu-N-double-positive cells (Fig. 4G) nor GFP- and CD-31-double-positive cells (Fig. 4I) were detected. Three-dimensional reconstruction of confocal image of double immunofluorescent staining for GFP and GFAP revealed co-localization of GFP and GFAP (Fig. 4I).

The numbers of GFP- and GFAP-double-positive cells (SCI+PBS: 0.6±0.4, SCI+G-CSF: 36.0±4.2) and GFP- and APC-double-positive cells (SCI+PBS: 0.6±0.3, SCI+G-CSF: 3.6±1.6) were larger in the SCI+G-CSF group (Figs. 5B, C, hatched columns, $p<0.05$) than in the SCI+PBS group (Figs. 5B, C, open columns).

To assess spinal cord tissue restoration, we performed luxol fast blue (LFB) staining. The average area of LFB-positive spared white matter was significantly larger in the SCI+G-CSF group than that in the SCI+PBS group (Fig. 6), indicating that G-CSF promoted restoration of spinal cord tissue.

Finally, we assessed the recovery of hind limb function using the motor function scale (Farooque et al., 2001), in which the maximum hind limb motor function scale is 13. All mice had a score of 13 before surgery, and the score dropped to 0 immediately after the spinal cord injury. Significant recovery of hind limb function was observed in mice from the SCI+G-CSF group (Fig. 6A, square) 4 weeks ($p<0.05$), 5 weeks and 6 weeks after injury ($p<0.01$) compared with the SCI+PBS group (Fig. 7A, circle). The average recovery score in the SCI+G-CSF group 6 weeks after injury was 4.7, indicating rhythmic bilateral hind limb stepping without weight bearing, whereas the average score in the SCI+PBS group was 3.1, indicating obvious bilateral hind limb motion without rhythmic stepping (Fig. 7B). Two mice in the SCI+G-CSF group showed the highest recovery score 6, indicating weight-bearing ability of hind limbs with abnormal walking (external rotation of one or both limbs and/or hip instability). In the Farooque's motor function scale system we used in the current study, score above 6 indicates weight support ability, which has significant impact in clinical situation.

3. Discussion

In the present study, we demonstrated that G-CSF promoted the migration of bone marrow-derived cells into the lesioned spinal cord and accelerated the recovery of hind limb function.

G-CSF has the potential to mobilize bone marrow cells into the peripheral blood. It is well known that G-CSF can increase the concentration of HSCs in the peripheral blood to that equaling or exceeding the concentration in bone marrow (Jansen et al., 2005). In addition to HSCs, cells of other lineages in the bone marrow, including mesenchymal stem cells, can be mobilized into the peripheral blood by G-CSF (Kawada et al., 2004). In the present study, G-CSF increased the number of GFP-positive/neutrophil antigen-negative spindle-shaped cells in the lesioned site 24 h after injury and a part of that population of cells expressed vimentin, which is a marker for cells of the mesenchymal lineage. In addition, GFP- and CD34-

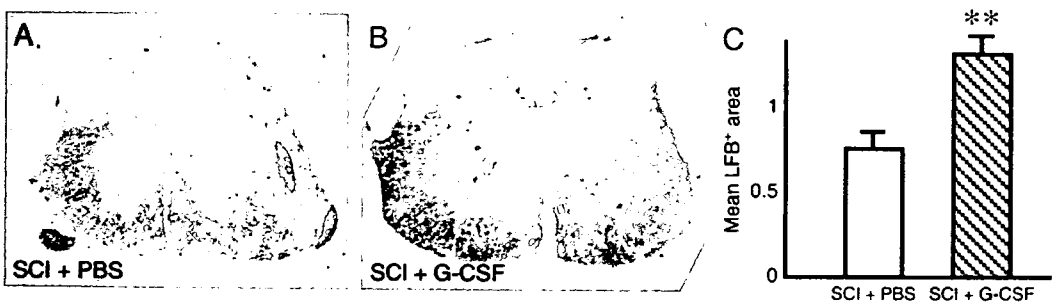

Fig. 6 – Luxol Fast Blue (LFB) staining to quantify white matter sparing. LFB-positive area in the SCI+G-CSF group (A) (C, hatched column) was significantly larger than that in the SCI+PBS group (B) (C, open column).

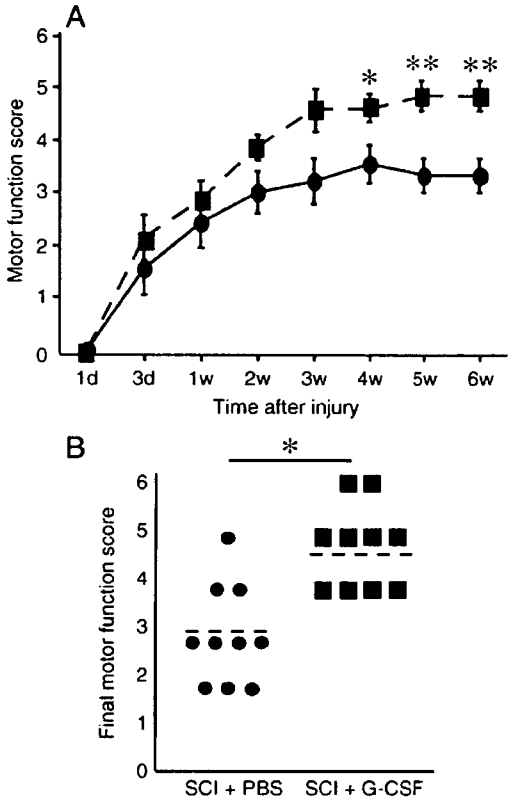

Fig. 7 – Hind limb functional assessment with the hind limb motor function scale (Farooque et al., 2001; Table 1). Time course of hind limb functional recovery (A) and comparison of final motor function score between the groups (B). Mice from the SCI+G-CSF group (square) showed significant recovery compared to mice from the SCI+PBS group (circle). Values are mean±S.E.M. *$p<0.05$, **$p<0.01$.

double-positive cells were detected near the lesion epicenter 1 week after injury. These findings may suggest that G-CSF promoted mobilization of bone marrow-derived stem cells, including HSCs and mesenchymal stem cells, both of which have the potential to restore damaged spinal cord tissue and to promote functional recovery, as we and others reported previously. The present results showed that G-CSF increased the number of bone marrow-derived cells in the injured spinal cord and promoted glial differentiation of bone marrow-derived cells in the chronic phase of spinal cord injury. These results may reflect the increase of G-CSF-mediated migration of bone marrow-derived stem cells into the lesioned spinal cord. In the present study, the differentiation of bone marrow-derived cells in the injured spinal cord was restricted to glial cells. It was reported that G-CSF promotes migration and differentiation into neurons of bone marrow-derived cells in normal and ischemic brain (Corti et al., 2002a; Kawada et al., 2006). A possible explanation is that the difference in the microenvironment between the brain and spinal cord and the difference between the ischemic and traumatic injury models cause a discrepancy between the results of the previous reports and the present results in the spinal cord injury model (Cao et al., 2001). Another possibility is that G-CSF modulated the environment in the injured spinal cord, including the cytokine expression profile (Zavala et al., 2002), resulting in enhancement of survival, proliferation and differentiation into cells of the neural lineage of bone marrow-derived stem cells that migrated into the lesioned site.

Hind limb function significantly improved in G-CSF-treated mice in the current study. Possible mechanisms of G-CSF-mediated functional recovery are as follows: 1) soluble factors secreted from bone marrow-derived stem cells that migrated into the lesioned spinal cord may ameliorate functional deficits. It is known that HSCs secrete growth factors that have neurotrophic properties (Takakura et al., 2000), and mesenchymal stem cells secrete interleukins and neurotrophic factors (Chopp and Li, 2002), by which HSCs and mesenchymal stem cells can contribute to the restoration of damaged central nervous tissue; 2) bone marrow-derived stem cells that were mobilized into the spinal cord by G-CSF into host spinal cord tissue. It has been reported that both HSCs (Cogle et al., 2004; Sigurjonsson et al., 2005) and mesenchymal stem cells (Tondreau et al., 2004) may have the potential to differentiate into neural cells, although the transdifferentiation of bone marrow cells is still controversial (Herzog et al., 2003). In addition to G-CSF-mediated differentiation into neural cells, G-CSF also increased the number of Mac-1-positive macrophages/microglia. Macrophages/microglia has the potential to scavenge cell debris around the lesioned site and to secrete neurotrophic factors, actions that can contribute to the restoration of the damaged spinal cord (Popovich, 2000; Bouhy et al., 2006).

Recently, it was reported that G-CSF- or GM-CSF-mediated mobilization of bone marrow-derived cells may promote spinal cord tissue restoration (Park et al., 2005 Urdzikova et al., 2006). However, their reports lack the direct evidence of bone marrow cell mobilization using bone marrow chimera mice. Moreover, in those reports, G-CSF or GM-CSF administration was initiated 1 week after injury, which is different from the present study. Further investigation is needed to elucidate the optimal time point of G-CSF-mediated bone marrow cell mobilization for spinal cord injury.

We also speculated that a direct neuroprotective effect of G-CSF may ameliorate functional deficits of spinal cord-injured mice. It is reported that G-CSF inhibits glutamate-induced neuronal death of cerebellar granule neurons *in vitro* and also inhibits ischemia-induced neuronal death in the rat brain *in vivo*, resulting in a decrease in infarction volume (Shäbitz et al., 2003; Schneider et al., 2005). These investigators also reported that the neuroprotective effect of G-CSF is mediated by the G-CSF receptor and its downstream signaling pathway. In the present study, there is a possibility that G-CSF may affect the spinal cord neurons and glial cells directly. Finally, suppression or modulation of cytokine expression by G-CSF may contribute to the restoration of the damaged spinal cord and functional recovery. It has been reported that G-CSF suppresses inflammatory cytokine expression of monocytes in vitro (Nishiki et al., 2004) and modulates inflammatory cytokine expression in experimental allergic encephalitis (Zavala et al., 2002). Inflammatory cytokines are thought to promote the progression of secondary injury in the acute phase of spinal cord injury. Further

investigation is needed to elucidate these mechanisms of action of G-CSF.

Regarding the clinical application of G-CSF for the treatment of spinal cord injury, G-CSF has some advantages over other treatments under investigation. First, G-CSF has already been approved as a safe drug, and it is widely used in clinics. Second, G-CSF-mediated mobilization of bone marrow-derived cells does not require injection of the cells directly into the lesioned spinal cord, thus avoiding additional trauma. Moreover, G-CSF-mediated mobilization of bone marrow-derived cells does not require harvesting and cultivation of any cells *in vitro*, resulting in the avoidance of associated risks including contamination, tumor formation, immunological rejection and ethical problems.

In conclusion, G-CSF promotes the migration of bone marrow-derived cells into the lesioned spinal cord and the recovery of hind limb function. The present results encourage the use of G-CSF to treat spinal cord injury, although further investigation is needed to advance G-CSF treatment for this clinical application.

4. Experimental procedure

4.1. *Bone marrow transplantation*

Bone marrow cells were collected from 8- to 12-week-old male green fluorescent protein transgenic mice (GFP Tg; Okabe et al., 1997). GFP Tg mice were euthanized with a pentobarbital overdose, and femurs and tibias were removed and placed in cold phosphate-buffered saline (PBS). After removal of the epiphyses of the femurs and tibias, the marrow was flushed out with PBS using a 26G needle attached to a syringe. A total of 6×10^6 bone marrow cells derived from GFP Tg mice were transplanted intravenously via the tail vein of lethally irradiated (10 Gy) female C57BL/6 mice (SLC, Hamamatsu, Japan). Four weeks after bone marrow transplantation, whole bone marrow cells were collected as mentioned above for fluorescence-activated cell-sorter (FACS) scanner analysis with FACScan (Becton Dickinson, San Jose, CA) to evaluate chimerism ($n=2$).

4.2. *Spinal cord injury and G-CSF treatment*

Four weeks after bone marrow transplantation, surgery and G-CSF treatment were performed. A total of 38 mice were used in the present study. Animals were divided into four groups, including spinal cord injury with G-CSF treatment (SCI + G-CSF group; $n=14$), spinal cord injury with vehicle control (SCI + PBS group; $n=14$), sham operation with G-CSF treatment (G-CSF group; $n=5$) and sham operation without G-CSF treatment (PBS group; $n=5$). Under halothane anesthesia, laminectomy was performed at the Th7–8 level, leaving the dura intact. The animals were then placed in a stereotaxic apparatus, and two adjustable forceps were applied to the spinous processes of both T6 and T9 to stabilize the spine. The dural tube was compressed with a steady load of 20 g for 5 min at the site of the Th7–8 laminectomy. The tip of the weight was a 1×2-mm rectangular plastic plate (Farooque et al., 2001). The mice were kept under a heating lamp until they regained consciousness. No pre- or post-operative antibiotics were given. Bladder function was observed during the first days after trauma for signs of urinary retention. Food and water were provided ad libitum before and after the experiments. The mice were kept in a temperature-controlled environment of 20 °C, and were exposed to alternate light and dark periods of 12 h. All animals were treated and cared for in accordance with the Chiba University School of Medicine guidelines pertaining to the treatment of experimental animals.

Immediately after injury, recombinant human G-CSF (200 μg/kg/day; kindly provided by Kirin Brewery Co. Ltd., Pharmatheutical Division, Tokyo, Japan) or vehicle alone (1% bovine serum albumin in PBS) was injected subcutaneously for 5 days in each group.

4.3. *Assessment of locomotor activity*

The functional recovery of hind limb of mice in the SCI + G-CSF ($n=10$) and SCI + PBS ($n=10$) groups was determined by measuring the hind limb motor function score as previously described by Farooque et al. (2001). Mice were allowed to move freely on the open field with rough surface for 5 min at each time tested. The hind limb movement of mice were videotaped and scored by two independent observers who were unaware of the treatment. Measurement of motor function was performed before surgery, 1 and 3 days and 1–6 weeks (once a week) after spinal cord injury. The scale ranged from 0 to 13, and scores were as shown in Table 1. In brief, score 0 means complete paralysis, scores 1–3 means movements of hind limbs without rhythmical stepping, scores 4 and 5 mean rhythmical motion of hind limbs without weight bearing ability, scores 6 and 7 mean weight bearing ability, scores 8–12

Table 1

Score	Criteria
0	No noticeable movements of the hind limbs.
1	Occasional, barely visible movements of any hind limb joint (hip, knee, or ankle).
2	Obvious movements of one or more joints in one hind limb but no forwards propulsive, stepping movements.
3	Obvious movements of one or more joints in both hind limbs but no forwards propulsive, stepping movements.
4	Stepping and forwards propulsive movement of one hind limb. No weight-bearing. Often external rotation of the hind limb.
5	Alternate stepping and forwards propulsive movements of both hind limbs but no weight-bearing ability. Often external rotation of hind limbs.
6	Weight-bearing ability of hind limbs but no normal walking (external rotation of one or both limbs and/or hip instability). The animals sweep one or both feet while walking (an obvious friction noise can be heard).
7	Weight-bearing ability of hind limbs, walks with a mild deficit (slight external rotation of one or both limbs and/or hip instability).
8	Normal movements except for reduced speed of walking.
9	Normal movements, ability to walk on a 2-cm wide bar.
10	Normal movements, ability to walk on a 1.5-cm wide bar.
11	Normal movements, ability to walk on a 1-cm wide bar.
12	Normal movements, ability to walk on a 7-mm wide bar.
13	Normal movements, ability to walk on a 5-mm wide bar.

means walking ability with increase of the hind limb gait width and score 13 means full recovery.

Mice in both the G-CSF and PBS groups were excluded from behavioral assessment, because they showed no apparent neurological deficit throughout the experimental period.

4.4. *Tissue preparation*

For histological evaluation, animals in all of the groups were perfused transcardially with 4% paraformaldehyde in PBS (pH 7.4) under pentobarbital anesthesia 1 day (n=4/group) and 6 weeks (n=10/group) after surgery. Three segments of spinal cords, including the lesion epicenter (T7–9) were removed and postfixed in the same fixative overnight, stored in 20% sucrose in PBS at 4 °C, and embedded in OCT compound (Sakura Finetechnical, Tokyo, Japan). The cryoprotected samples were frozen and kept at −80 °C until use. The samples were cut into serial 20-μm transverse sections with a cryostat and mounted onto poly-L-lysine-coated slides (Matsunami, Tokyo, Japan).

4.5. *Histological assessment and immunohistochemistry*

We performed luxol fast blue (LFB) staining to measure the area of spared white matter.

Immunohistochemistry was performed to identify the distribution and cell types of GFP-expressing bone marrow-derived cells, as previously described (Hashimoto et al., 2003; Kamada et al., 2005). The specificity of the staining procedures was controlled by omitting primary or secondary antibodies. The primary antibodies used were as follows: rat monoclonal anti-CD34 antibody (CD34, 1: 200, Acris Antibodies GmbH, Hiddenhausen, Germany), mouse monoclonal anti-neuronal nuclear antigen antibody (NeuN, 1:800, Chemicon Int., Temecula, CA) for neurons, mouse monoclonal anti-glial fibrillary acidic protein antibody (GFAP, 1:1600, Sigma) for astrocytes, mouse monoclonal anti-adenomatous polyposis coli antibody (APC, 1:800, Calbiochem, San Diego, CA) for oligodendrocytes, rat monoclonal anti-CD11b antibody (Mac-1, 1: 400, Serotec, Oxford, UK) for macrophages/microglia, rat monoclonal anti-neutrophil antibody (1:400, Serotec) for infiltrating neutrophils, mouse monoclonal anti-nestin (1:800, Chemicon Int.) for neural stem/progenitor cells and rat monoclonal anti-CD31 antibody (Pharmingen, San Jose, CA) for endothelial cells. The sections were reacted with cell-type marker antibodies overnight at 4 °C. After 3 10-min washes with PBS, the sections were reacted with Alexa 594-labeled anti-rabbit, anti-mouse or anti-rat IgG antibody (Molecular Probes) at room temperature for 1 h. The positive signals were observed by fluorescence microscope (ECLIPSE E600; Nikon, Tokyo, Japan). We also used Zeiss LSM 510 confocal laser scanning microscope to observe GFP- and GFAP-double-positive cells and GFP- and CD34-positive cells.

For quantitative analysis of the spared white matter area and the differentiation of bone marrow-derived cells that migrated into the spinal cord, every fifth 20-μm transverse sections (100 μm apart) were picked up from either 300–900 μm rostral or 300–900 μm caudal to the lesion epicenter. Sections near the lesion epicenter were excluded from histological and immunohistochemical assessment because the tissue destruction was too severe to perform quantitative analysis in that area. Six sections were taken from the spinal cords of mice from each group. The LFB-positive area was calculated using Scion Image computer analysis software (Scion Corporation, Frederick, MA). The sections were immunostained with antibodies to markers for each cell lineage, as described above. The numbers of double-positive cells and GFP-positive cells were summed.

4.6. *Statistical analysis*

GFP-positive cell count, double immunofluorescence study, LFB-positive area and the final motor function score were subjected to the Student's t-test. Motor function scores were subjected to Repeated Measures ANOVA followed by post hoc test using Scheffe's F test. Data are presented as mean values ± S.E. Values of $p<0.05$ were considered statistically significant.

Acknowledgments

We are grateful to Kirin Brewery Co. Ltd., Pharmatheutical Division for their kind gift of G-CSF. This work was supported by grants-in-aid for Scientific Research from the Ministry of Education, Science and Culture of Japan (16591473) and grant from the General Insurance Association of Japan.

REFERENCES

Bacigalupo, A., 2004. Mesenchymal stem cells and haematopoietic stem cell transplantation. Best Pract. Res., Clin. Haematol. 17, 387–399.

Bouhy, D., Malgrange, B., Multon, S., Poirrier, A.L., Scholtes, F., Schoenen, J., Franzen, R., 2006. Delayed GM-CSF treatment stimulates axonal regeneration and functional recovery in paraplegic rats via an increased BDNF expression by endogenous macrophages. FASEB J. 20, 1239–1241.

Cao, Q.L., Zhang, Y.P., Howard, R.M., Walters, W.M., Tsoulfas, P., Whittemore, S.R., 2001. Pluripotent stem cells engrafted into the normal or lesioned adult rat spinal cord are restricted to a glial lineage. Exp. Neurol. 167, 48–58.

Chopp, M., Li, Y., 2002. Treatment of neural injury with marrow stromal cells. Lancet Neurol. 1, 92–100.

Chopp, M., Zhang, X.H., Li, Y., 2000. Spinal cord injury in rat: treatment with bone marrow stromal cell transplantation. NeuroReport 11, 3001–3005.

Cogle, C.R., Yachnis, A.T., Laywell, E.D., Zander, D.S., Wingard, J.R., Steindler, D.A., Scott, E.W., 2004. Bone marrow transdifferentiation in brain after transplantation: a retrospective study. Lancet 363, 1432–1437.

Corti, S., Locatelli, F., Strazzer, S., Salani, S., Del Bo, R., Soligo, D., Bossolasco, P., Bersolin, N., Scarlato, G., Comi, C.P., 2002a. Modulated generation of neuronal cells from bone marrow by expansion and mobilization of circulating stem cells with in vivo cytokine treatment. Exp. Neurol. 177, 443–452.

Corti, S., Locatelli, F., Donadoni, C., Strazzers, S., Salani, S., Del Bo, R., Caccialanza, M., Bresolin, N., Scarlato, G., Comi, G.P., 2002b. Neuroectodermal and microglial differentiation of bone marrow cells in the mouse spinal cord and sensory ganglia. J. Neurosci. Res. 70, 721–733.

Farooque, M., Isaksson, J., Olsson, Y., 2001. Improved recovery after spinal cord injury in neuronal nitric oxide synthase-deficient mice but not in TNF-alpha-deficient mice. J. Neurotrauma 18, 105–114.

Hashimoto, M., Koda, M., Ino, H., Murakami, M., Yamazaki, M., Moriya, H., 2003. Upregulation of osteopontin expression in rat spinal cord microglia after traumatic injury. J. Neurotrauma 20, 287–296.

Herzog, E.L., Chai, L., Krause, D.S., 2003. Plasticity of marrow-derived stem cells. Blood 102, 3483–3493.

Hofstetter, C.P., Schwarz, E.J., Hess, D., Widenfalk, J., El Manira, A., Prockop, D.J., Olson, L., 2002. Marrow stromal cells form guiding strands in the injured spinal cord and promote recovery. Proc. Natl. Acad. Sci. U. S. A. 19, 2199–2204.

Jansen, J., Hanks, S., Thompson, J.M., Dugan, M.J., Akard, L.P., 2005. Transplantation of hematopoietic stem cells from the peripheral blood. J. Cell. Mol. Med. 9, 37–50.

Kamada, T., Koda, M., Dezawa, M., Yoshinaga, K., Hashimoto, M., Koshizuka, S., Nishio, Y., Moriya, H., Yamazaki, M., 2005. Transplantation of Schwann cells derived from bone marrow stromal cells promotes axonal regeneration and functional recovery after complete transection of adult rat spinal cord. J. Neuropathol. Exp. Neurol. 64, 37–45.

Kawada, H., Fujita, J., Kinjo, K., Matsuzaki, Y., Tsuma, M., Miyatake, H., Muguruma, Y., Tsuboi, K., Itabashi, Y., Ikeda, Y., Ogawa, S., Okano, H., Hotta, T., Ando, K., Fukuda, K., 2004. Nonhematopoietic mesenchymal stem cells can be mobilized and differentiate into cardiomyocytes after myocardial infarction. Blood 104, 3581–3587.

Kawada, H., Takizawa, S., Takanashi, T., Morita, Y., Fujita, J., Fukuda, K., Takagi, S., Okano, H., Ando, K., Hotta, T., 2006. Administration of hematopoietic cytokines in the subacute phase after cerebral infarction is effective for functional recovery facilitating proliferation of intrinsic neural stem/progenitor cells and transition of bone marrow-derived neuronal cells. Circulation 113, 701–710.

Koda, M., Okada, S., Nakayama, T., Koshizuka, S., Kamada, T., Nishio, Y., Someya, Y., Yoshinaga, K., Okawa, A., Moriya, H., Yamazaki, M., 2005. Hematopoietic stem cell and marrow stromal cell for spinal cord injury in mice. NeuroReport 16, 1763–1767.

Koshizuka, S., Okada, S., Okawa, A., Koda, M., Murasawa, M., Hashimoto, M., Kamada, T., Yoshinaga, K., Murakami, M., Moriya, H., Yamazaki, M., 2004. Transplanted hematopoietic stem cells from bone marrow differentiate into neural lineage cells and promote functional recovery after spinal cord injury in mice. J. Neuropathol. Exp. Neurol. 63, 64–72.

Nicola, N.A., Metcalf, D., Matsumoto, M., Johonson, G.R., 1983. Purification of a factor inducing differentiation in murine myelomonocytic leukemia cells. Identification as granulocyte colony-stimulating factor. J. Biol. Chem. 258, 9017–9023.

Nishiki, S., Hato, F., Kamata, N., Sakamoto, E., Hasegawa, T., Kimura-Eto, A., Hino, M., Kitagawa, S., 2004. Selective activation of STAT 3 in human monocytes stimulated by G-CSF: implication in inhibition of LPS-induced TNF-α production. Am. J. Physiol.: Cell Physiol. 286, 1302–1311.

Okabe, M., Ikawa, M., Kominami, K., Nakanishi, T., Nishimune, Y., 1997. 'Green mice' as a source of ubiquitous green cells. FEBS Lett. 407, 313–319.

Orlic, D., Kajstura, J., Chimenti, S., Limana, F., Jakoniuk, I., Quaini, F., Nadal-Ginard, B., Bodine, D.M., Leri, A., Anversa, P., 2001. Mobilized bone marrow cells repair the infarcted heart, improving function and survival. Proc. Natl. Acad. Sci. U. S. A. 98, 10344–10349.

Park, H.C., Shim, Y.S., Ha, Y., Yoon, S.H., Park, S.R., Choi, B.H., Park, H.S., 2005. Treatment of complete spinal cord injury patients by autologous bone marrow cell transplantation and administration of granulocyte–macrophage colony stimulating factor. Tissue Eng. 11, 913–922.

Popovich, P.G., 2000. Immunological regulation of neuronal degeneration and regeneration in the injured spinal cord. Prog. Brain Res. 128, 43–58.

Roberts, A.W., 2005. G-CSF: a key regulator of neutrophil production, but that's no all! Growth Factors 23, 33–41.

Schneider, A., Krüger, C., Steigleder, T., Weber, D., Pitzer, C., Laage, R., Aronowski, J., Maurer, M.H., Gassler, N., Mier, W., Hasselblatt, M., Kollmar, R., Schwab, S., Sommer, C., Bach, A., Kuhn, H.G., Shäbitz, W.R., 2005. The hematopoietic factor G-CSF is a neuronal ligand that counteracts programmed cell death and drives neurogenesis. J. Clin. Invest. 115, 2083–2098.

Shäbitz, W.R., Kollmar, R., Schwaninger, M., Juettler, E., Bardutzky, J., Schölzke, M.N., Sommer, C., Schwab, S., 2003. Neuroprotective effect of granulocyte colony-stimulating factor after focal cerebral ischemia. Stroke 34, 745–751.

Sigurjonsson, O.E., Perreault, M.C., Egeland, T., Glover, J.C., 2005. Adult human hematopoietic stem cells produce neurons efficiently in the regenerating chicken embryo spinal cord. Proc. Natl. Acad. Sci. U. S. A. 102, 5227–5232.

Takakura, N., Watanabe, T., Suenobu, S., Yamada, Y., Noda, T., Ito, Y., Satake, M., Suda, T., 2000. A role for hematopoietic stem cells in promoting angiogenesis. Cell 102, 199–209.

Tondreau, T., Lagneaux, L., Dejeneffe, M., Massy, M., Mortier, C., Delforge, A., Bron, D., 2004. Bone marrow-derived mesenchymal stem cells already express specific neural proteins before any differentiation. Differentiation 72, 319–326.

Urdzikova, L., Jendelova, P., Glogarova, K., Burian, M., Hajek, M., Sykova, E., 2006. Transplantation of bone marrow stem cells as well as mobilization by granulocyte-colony stimulating factor promotes recovery after spinal cord injury in rats. J. Neurotrauma 23, 1379–1391.

Wu, S., Suzuki, Y., Ejiri, Y., Noda, T., Bai, H., Kitada, M., Kataoka, K., Ohta, M., Chou, H., Ide, C., 2003. Bone marrow stromal cells enhance differentiation of cocultured neurosphere cells and promote regeneration of injured spinal cord. J. Neurosci. Res. 72, 343–351.

Zavala, F., Abad, S., Ezine, S., Taupin, V., Masson, A., Bach, J.F., 2002. G-CSF therapy of ongoing experimental allergic encephalomyelitis via chemokine- and cytokine-based immune deviation. J. Immunol. 168, 2011–2019.

J Neuropathol Exp Neurol
Copyright © 2007 by the American Association of Neuropathologists, Inc.

Vol. 66, No. 8
August 2007
pp. 724–731

ORIGINAL ARTICLE

Granulocyte Colony-Stimulating Factor Attenuates Neuronal Death and Promotes Functional Recovery After Spinal Cord Injury in Mice

Yutaka Nishio, MD, PhD, Masao Koda, MD, PhD, Takahito Kamada, MD, PhD, Yukio Someya, MD, PhD, Ryo Kadota, MD, Chikato Mannoji, MD, Tomohiro Miyashita, MD, Seiji Okada, MD, PhD, Akihiko Okawa, MD, PhD, Hideshige Moriya, MD, PhD, and Masashi Yamazaki, MD, PhD

Abstract

Granulocyte colony-stimulating factor (G-CSF) is a protein that stimulates differentiation, proliferation, and survival of granulocytic lineage cells. Recently, a neuroprotective effect of G-CSF was reported in a model of cerebral infarction. The aim of the present study was to elucidate the potential therapeutic effect of G-CSF for spinal cord injury (SCI) in mice. We found that G-CSF is neuroprotective against glutamate-induced cell death of cerebellar granule neurons in vitro. Moreover, we used a mouse model of compressive SCI to examine the neuroprotective potential of G-CSF in vivo. Histologic assessment with cresyl violet staining revealed that the number of surviving neurons in the injured spinal cord was significantly increased in G-CSF-treated mice. Immunohistochemistry for neuronal apoptosis revealed that G-CSF suppressed neuronal apoptosis after SCI. Moreover, administration of G-CSF promoted hindlimb functional recovery. Examination of signaling pathways downstream of the G-CSF receptor suggests that G-CSF might promote functional recovery by inhibiting neuronal apoptosis after SCI. G-CSF is currently used in the clinic for hematopoietic stimulation, and its ongoing clinical trial for brain infarction makes it an appealing molecule that could be rapidly placed into trials for patients with acute SCI.

Key Words: Apoptosis, Neuroprotection, Secondary injury.

From the Department of Orthopaedic Surgery (YN, TK, YS, RK, CM, TM, AO, HM, MY), Graduate School of Medicine, Chiba University, Chiba Japan; Department of Orthopaedic Surgery (MK), Togane Hospital, Chiba, Japan; and Division of Hematopoiesis Center for AIDS Research (SO), Kumamoto University, Kumamoto, Japan.

Send correspondence and reprint requests to: Masashi Yamazaki, MD, PhD, Department of Orthopaedic Surgery, Chiba University Graduate School of Medicine, 1-8-1 Inohana, Chuo-ku, Chiba 260-8670 Japan; E-mail: masashiy@faculty.chiba-u.jp

This work was supported by a grant-in-aid for Scientific Research from the Ministry of Education, Science and Culture of Japan (16591473) and by a medical research grant from of the General Insurance Association of Japan.

INTRODUCTION

The pathologic sequelae that follow acute spinal cord injury (SCI) are divided into 2 broad chronologic events: the primary injury and the secondary injury (1). The primary injury encompasses the focal destruction of neural tissue caused by direct mechanical trauma. This initial insult then instigates a progressive wave of secondary injury, which exacerbates the injury to the spinal cord via the activation of pathophysiologic mechanisms. Because this wave of secondary injury leads to the apoptotic death of neuronal and glial cells left intact by the initial trauma, it is a major impediment to functional recovery after SCI (1). Thus, apoptosis of neurons and glial cells after acute SCI is one of the main therapeutic targets for various kinds of drug therapies.

Granulocyte colony-stimulating factor (G-CSF) is a 19.6-kDa glycoprotein that was identified initially as a serum component that induces differentiation of the murine myelomonocytic leukemic cell line and is capable of inducing the survival, proliferation, and differentiation of cells of neutrophil granulocyte precursors (2, 3). In addition, G-CSF inhibits apoptosis of postmitotic neutrophil lineage cells. This effect results in increased numbers of circulating neutrophils, which is used for neutropenia in clinical situations. In addition to its antiapoptotic effect for neutrophil, it was recently reported that G-CSF has the potential to inhibit apoptosis of postmitotic cells of nonhematopoietic lineage. For instance, G-CSF suppresses apoptosis of cardiomyocytes in an acute myocardial infarction model (4). It is supposed that G-CSF activates common antiapoptotic machinery, which is conserved among the different lineage cells. In the CNS, apoptosis of neurons can also be suppressed by G-CSF. Recent reports showed that G-CSF attenuates glutamate-induced neuronal death in vitro and protects neurons after stroke in vivo (5–7). These lines of evidence show the antiapoptotic potential of G-CSF in the CNS, raising the possibility that G-CSF may also act as a neuroprotectant in acute SCI.

In the current study, we tested the hypothesis that G-CSF could attenuate neuronal apoptosis and promote functional recovery after SCI.

MATERIALS AND METHODS

Cell Culture

Cerebellar granule neurons (CGNs) were prepared from postnatal day 7 mice. Fresh cerebella were dissected, and the tissue was dissociated with trypsin (2.5 mg/mL; Invitrogen, Carlsbad, CA) and DNase I (0.3 mg/mL; Roche Applied Science, Indianapolis, IN). Cells were plated on poly-L-lysine-coated chamber slides (Lab-Tek Chamber Slides Permanox; Nalge Nunc International, Rochester, NY) or 6-cm dishes at a density of 7.0×10^4 cells/cm^2 in Dulbecco's modified Eagle's medium Gibco BRL (Grand Island, NY), supplemented with 10% fetal bovine serum, penicillin-streptomycin (100 units/mL penicillin G sodium, 100 μg/mL streptomycin sulfate; Invitrogen), and 0.02 M HEPES. After 16 hours in culture, the medium was replaced with Dulbecco's modified Eagle's medium supplemented with penicillin-streptomycin, 20 mM HEPES, N2 supplement (0.01%; Invitrogen), KCl (20 mM), fibronectin (10 μg/mL), and cytosine arabinoside (1.0 μM). Cells were maintained in a humidified atmosphere containing 5% CO_2 at 37°C. Experiments on CGNs were performed after 7 days in culture.

Immunocytochemistry and Immunohistochemistry

To detect the G-CSF receptor (G-CSFR), immunocytochemical staining on cultured CGNs and immunohistochemistry on intact mouse spinal cord sections were performed. For histologic sections, animals were perfused transcardially with 4% paraformaldehyde in PBS under deep pentobarbital anesthesia. Spinal cord tissue was fixed overnight by immersion in 4% paraformaldehyde in PBS and then immersed for 48 hours in 20% sucrose in PBS at 4°C. The tissue was embedded in O.C.T. compound (Tissue-Tek; Sakura Finetech. Tokyo, Japan), frozen on dry ice, and sectioned on a cryostat. Axial sections (12 μm thick) were mounted onto poly-L-lysine-coated glass slides (Matsunami, Tokyo, Japan) and dried for 48 hours at room temperature. Immunocytochemistry and immunohistochemistry were performed as described previously (8). Briefly, cultured CGNs on chamber slides were washed 3 times with PBS, fixed with 4% paraformaldehyde for 10 minutes, and then washed 3 times with PBS. Histologic sections of mouse spinal cord were rehydrated with 0.3% Triton X in PBS for 1 hour and washed 3 times with PBS. Slides were then incubated with blocking solution (0.05 M Tris HCl, pH 7.6, 1% bovine serum albumin, Block Ace [Yukijirusi, Sapporo, Japan], 0.15 M NaCl, and 0.1% Tween 20) for 30 minutes at room temperature. After blocking, the slides were incubated with anti G-CSF receptor rabbit polyclonal antibody (1:100 dilution; Santa Cruz Biotechnology, Santa Cruz, CA) and anti-neuronal nuclei mouse monoclonal antibody (Neu-N) (1:400 dilution; Chemicon International, Inc., Temecula, CA) overnight at 4°C. The slides were then washed 3 times for 5 minutes with PBS and incubated with secondary antibodies (goat anti-rabbit, Alexa Fluor 594, 1:800 dilution and goat anti-mouse, Alexa Fluor 388, 1:800 dilution; Molecular Probes, Eugene, OR) for 30 minutes at room temperature. The slides were then washed 3 times with PBS and analyzed by confocal laser scanning microscopy (LSM5 PASCAL; Carl Zeiss, Germany, Oberkochen).

Reverse Transcriptase-Polymerase Chain Reaction

To detect expression of G-CSFR mRNA in CGNs and spinal cord tissue, we performed reverse transcriptase (RT)-polymerase chain reaction (PCR). Total RNA was extracted from cultured CGNs or intact spinal cord tissue using TRIzol reagent (Gibco Life Technologies, Rockville, MD) according to the manufacturer's protocol. cDNAs were prepared by reverse transcription from 2.5 μg of total RNA using the Superscript II RT Preamplification System (Gibco Life Technologies) with an oligo $(dT)_{12\text{-}18}$ primer. PCR was performed with 2.0 μL of cDNA in a 50-μL reaction mixture containing 200 nM dNTP, 0.5 U of Extra Taq DNA polymerase (Takara, Tokyo, Japan), and forward and reverse PCR primers. Sequences of both primers were 5′-GTACTCTTGTCCACT ACCTGT-3′ and 5′-CAAGATA-CAAGGACCCCCAA-3′ for G-CSFR (accession number M58288). The following conditions were used for PCR amplification: after denaturation at 94°C for 5 minutes, the reaction was carried out at 94°C for 1 minute, 58°C for 1 minute, and 72°C for 1 minute (40 cycles). The resulting 567-base pair product was analyzed on a 1% agarose gel.

Cell Culture Experiment

After 7 days in culture, CGNs were treated with glutamate (100 μM) for 6 hours to induce cell death. Recombinant human G-CSF was provided by KIRIN Brewery (Tokyo, Japan). Neuronal death was detected by double staining with propidium iodide and calcein using a Live/Dead Double Staining Kit (MBL, Nagoya, Japan). The ratio of dead cells to total cells was calculated (number of dead cells/total cells) and compared between each group. G-CSF was added to the culture medium of glutamate-treated CGN in different concentrations (i.e. 0, 10, and 100 ng/mL) to assess the dose dependency of its neuroprotective effects. G-CSFR activation was blocked by addition of anti G-CSFR antibody (30 minutes before glutamate treatment; 2 μg/mL of antibodies SC 9173 and SC694; Santa Cruz Biotechnology) to examine the specificity of G-CSF effects on attenuation of CGN cell death.

Signaling pathways downstream of G-CSFR activation were blocked with specific inhibitors as follows: AG490 (100 nM, a specific Janus kinase 2 [JAK2]/signal transducer and activator of transcription [STAT] inhibitor; Calbiochem, San Diego, CA), wortmannin (50 nM, a specific phosphatidylinositol 3-kinase [PI3K] inhibitor; Calbiochem), and PD98059 (0.2–20 μM), a specific inhibitor of Ras/mitogen-activated protein kinase. The inhibitors were added to the culture medium 30 minutes before glutamate treatment. After 6 hours of incubation, cell death was determined as described above.

Western Blot Analysis

To determine the precise mechanism of the neuroprotective action of G-CSF, Western blot analysis was

TABLE. Measurement of Motor Function Before and After Spinal Cord Injury

Score	Criteria
0	No noticeable movements of the hindlimbs.
1	Occasional, barely visible movements of any hindlimb joint (hip, knee, or ankle).
2	Obvious movements of 1 or more joints in 1 hindlimb but no forward propulsive, stepping movements.
3	Obvious movements of 1 or more joints in both hindlimbs but no forward propulsive, stepping movements.
4	Stepping and forward propulsive movement of 1 hindlimb. No weight-bearing. Often external rotation of the hindlimb.
5	Alternate stepping and forward propulsive movements of both hindlimbs but no weight-bearing ability. Often external rotation of hindlimbs.
6	Weight-bearing ability of hindlimbs but no normal walking (external rotation of 1 or both limbs and/or hip instability). The animals sweep 1 or both feet while walking (an obvious friction noise can be heard).
7	Weight-bearing ability of hindlimbs, walks with a mild deficit (slight external rotation of 1 or both limbs and/or hip instability).
8	Normal movements except for reduced speed of walking.
9	Normal movements, ability to walk on a 2-cm-wide bar.
10	Normal movements, ability to walk on a 1.5-cm-wide bar.
11	Normal movements, ability to walk on a 1-cm-wide bar.
12	Normal movements, ability to walk on a 7-mm-wide bar.
13	Normal movements, ability to walk on a 5-mm-wide bar.

performed as described previously (9). Briefly, after washing with PBS, cultured CGNs were lysed in homogenization buffer (0.05 M Tris-HCl, pH 7.6, 2% Triton X, and 0.5% protease inhibitor cocktail [Sigma, St. Louis, MO]) at 37°C for 15 minutes. Homogenates were centrifuged at 10,000 x *g* for 5 minutes at 4°C. Samples were stored at –80°C until use. The protein concentration of the samples was determined by the Bradford method. Samples containing 50 μg of protein were electrophoresed on 8% or 12% sodium dodecyl sulfate-polyacrylamide gels, followed by transfer to polyvinylidene difluoride membranes (Hybond-P; Amersham, Piscataway, NJ). Phosphorylated STAT3 (pSTAT3) and Bcl-2 were detected with the anti-pSTAT3 antibody (1:100; Cell Signaling Technology, Inc., Danvers, MA) and anti-Bcl-2 antibody (1:100; Santa Cruz Biotechnology) followed by a peroxidase-conjugated anti-rabbit IgG antibody and anti-mouse IgG antibody (1:2,500; Amersham), respectively. The signal was developed with chemiluminescence (ECL Plus Kit; Amersham). After signal detection, the blots were stripped and reblotted with anti-STAT 3 antibody (1:1,000; Cell Signaling) and anti-actin antibody (1:500, Santa-Cruz) as internal controls.

Surgery and Drug Treatment

Tissue samples were obtained from 9- to 10-week-old female BALBc/Cr mice (18–21 g, average weight 19.5 g; SLC, Hamamatsu, Japan). Animals were anesthetized with 1% to 1.2% halothane in 0.5 L/min oxygen. After laminectomy (T7–8 level), the animals were placed in a stereotaxic apparatus and their spines were fixed with forceps. Compressive SCI was produced at the T7–8 level using a compression rod. The tip of the weight was a 1-mm × 2-mm rectangular plastic plate (10), and the static load (20 g) was applied for 5 minutes. Food and water were given ad libitum. All animals were treated and cared for in accordance with the Chiba University School of Medicine guidelines pertaining to the treatment of experimental animals.

The mice were randomly divided into 2 groups (G-CSF group and control group). The G-CSF group mice were subcutaneously injected with recombinant human G-CSF (200 μg/kg/day) for 5 days. The control group was injected with vehicle (1% bovine serum albumin in PBS) only.

Tissue Preparation and Immunohistochemical and Histologic Assessments

Animals were killed at 1 day, 3 days, and 6 weeks after SCI. After transcardiac perfusion, spinal cords were dissected out and 12-μm-thick serial sections were made as described above. Every fifth sections (60 μm apart) were used for histologic (6 weeks after injury) and immunohistochemical (1 day and 3 days after injury) examinations.

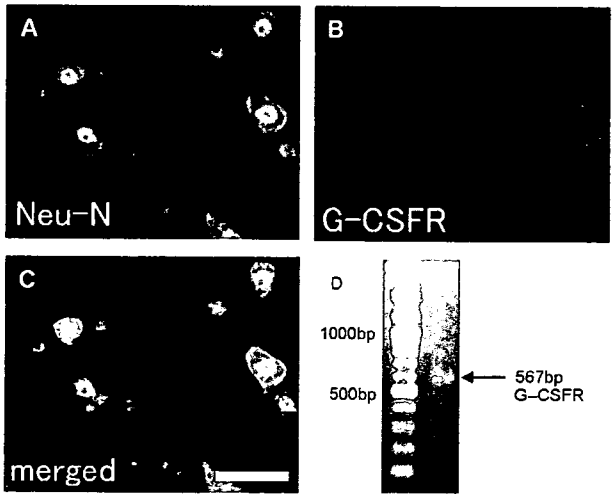

FIGURE 1. Granulocyte colony-stimulating factor receptor (G-CSFR) expression in mouse intact spinal cord. Immunofluorescence staining for **(A)** anti-neuronal nuclei mouse monoclonal antibody, a marker for neuron (green), **(B)** G-CSFR, and **(C)** merged view. G-CSFR expression was predominantly neuronal in mouse spinal cord. **(D)** Reverse transcriptase-polymerase chain reaction for mouse G-CSFR. Expression of G-CSFR mRNA was detected in mouse intact spinal cord with an expected size of 567 base pairs. Scale bar = **(A–C)** 50 μm.)

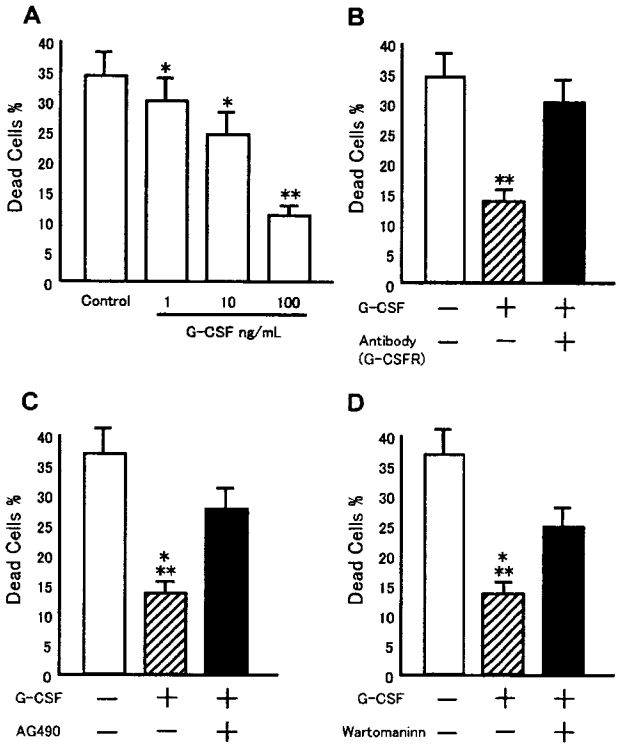

FIGURE 2. Granulocyte colony-stimulating factor (G-CSF) attenuates glutamate-induced neuronal death of cultured cerebellar granule neurons (CGNs). CGNs were exposed to glutamate (100 μM), and G-CSF was added to the culture medium. Viability of CGNs was evaluated with a Live/Dead Double Staining Kit. Granulocyte colony-stimulating factor attenuated glutamate-induced cell death of CGNs in a dose-dependent manner **(A)**. At the G-CSF concentration of 100 ng/mL, the neuroprotective effect was most apparent. Pretreatment of CGNs with anti G-CSFR antibody abolished G-CSF-mediated neuroprotection against glutamate-induced neuronal death **(B)**. Both the JAK2 inhibitor AG490 and the PI3K inhibitor wortmannin partially abolished G-CSF-mediated neuroprotection **(C, D)**. Data are expressed as means ± SE. *, significant difference compared with control ($p < 0.05$); **, significant difference compared with control ($p < 0.01$).

Then, 10 sections were picked up from both the rostral and caudal segments to the lesion epicenter and were used for histologic and immunohistochemical examinations. Sections near the lesion epicenter (from 300 μm rostral to 300 μm caudal) were excluded from immunohistochemical and histologic assessment because the tissue destruction was too severe to count neurons precisely in that area. Therefore, the analyses covered the area from either 300 to 900 μm rostral or 300 to 900 μm caudal to the lesion epicenter.

Immunohistochemistry for apoptotic cells was performed as described above to quantify neuronal apoptosis in the injured spinal cord. Mouse Neu-N antibody (1:400 dilution) was used as a neuronal specific marker, and rabbit anti-cleaved caspase-3 antibody (1:800 dilution; Genzyme/Techne, Minneapolis, MN) was used as a marker for apoptotic cells. Secondary antibodies were as follows: goat anti-mouse Alexa Fluor 488 and goat anti-rabbit Alexa Fluor 594 (1:800 dilution). The number of apoptotic neurons was determined by counting cells that were double positive for Neu-N and cleaved caspase-3. Neuronal survival was assessed 6 weeks after injury using cresyl violet staining.

Behavioral Testing for Recovery of Hindlimb Motor Function

The functional recovery of hindlimb was determined by measuring the hindlimb motor function score as described previously by Farooque et al (10). Mice were allowed to move freely in an open field with a rough surface for 5 minutes at each time tested. The hindlimb movements of mice were videotaped and scored by 2 independent observers who were unaware of the treatment group. Measurement of motor function was performed before surgery and 1 and 3 days and 1 to 6 weeks (once a week) after SCI. The scale ranged from 0 to 13, and scores are shown in the Table. In brief, a score of 0 indicates complete paralysis, a score of 1 to 3 indicates movement of hindlimbs without rhythmical stepping, a score of 4 to 5 indicates rhythmical motion of hindlimbs without weight-bearing ability, a score of 6 to 7 indicates weight-bearing ability, a score of 8 to 12 indicates walking ability with an increase in the hindlimb gait width, and a score of 13 indicates full recovery.

Statistical Analysis

Motor function scores were subjected to repeated measures analysis of variance followed by post hoc test using the Scheffé F-test. The final motor function score was statistically analyzed using the Mann-Whitney U-test. The neuron survival counts and apoptotic neuron counts were subjected to the Student *t*-test. Data are presented as mean

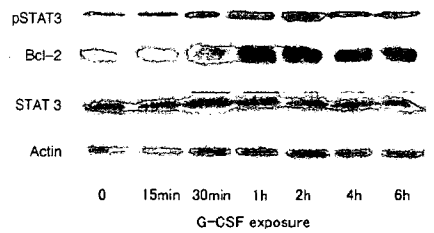

FIGURE 3. Western blot analysis for signaling molecules downstream of granulocyte colony-stimulating factor (G-CSF) receptor in cultured cerebellar granule neurons (CGNs). Cultured CGNs were exposed to G-CSF (100 ng/mL) and expression of phosphorylated signal transducer and activator of transcription 3 (pSTAT3) and Bcl-2 was detected by Western blot. The level of pSTAT3 increased by 15 minutes after G-CSF exposure, peaked 1 or 2 hours after exposure and then decreased after 6 hours. The level of Bcl-2 increased by 30 minutes after G-CSF exposure and remained elevated for 6 hours. There was no change in the expression levels of total STAT3 and actin, showing equal protein sample loading.

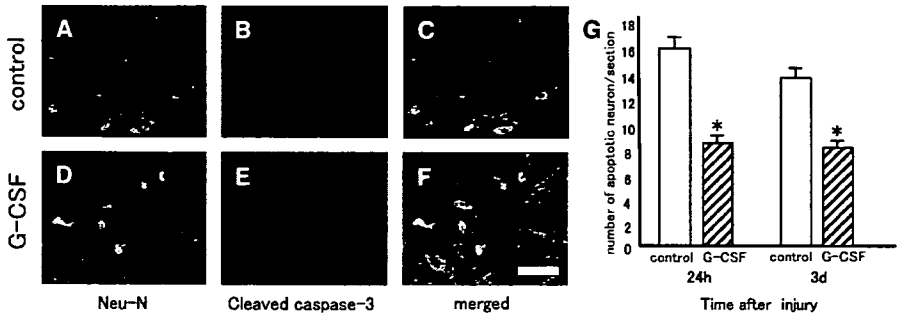

FIGURE 4. Immunohistochemical assessment of neuronal apoptosis in the acute phase after spinal cord injury. Double immunofluorescence staining for anti-neuronal nuclei mouse monoclonal antibody (Neu-N), a marker for neuron (green) (**(A, D)** and cleaved caspase-3 (red) **(B, E)** and the merged views **(C, F)**. **(A–C)** are the control group, and **(D–F)**) are the G-CSF-treated group. The number of apoptotic neurons (cells double positive for Neu-N and cleaved caspase-3) in the G-CSF group (hatched columns) was significantly smaller than that in the control group (open columns) at 24 hours and 3 days after injury. Data are expressed as means ± SE. *, significant difference ($p < 0.05$). Scale bar = 50 μm.

values ± SE. Values of $p < 0.05$ were considered statistically significant.

RESULTS

Granulocyte Colony-Stimulating Factor Receptor Expression in Vitro and in Vivo

In cultured CGNs, G-CSFR was detected by immunocytochemistry (not shown) and G-CSFR mRNA was detected by RT-PCR (not shown). Similarly, immunohistochemistry on intact mouse spinal cord sections revealed G-CSFR expression on Neu-N-positive neurons (Fig. 1A–C), and RT-PCR on intact mouse spinal cord showed G-CSFR mRNA expression (Fig. 1D). These data indicate that G-CSFR is expressed by neurons in vitro and in vivo (in spinal cord).

Cell Culture Experiment

To examine neuroprotection against glutamate-induced neuronal death, G-CSF was administered to cultured CGNs simultaneously with glutamate. The results showed that G-CSF significantly decreased glutamate-induced neuronal death in a dose-dependent manner, with a concentration of 100 ng/mL exhibiting the optimal neuroprotective effect (Fig. 2A).

To examine the specificity of G-CSF-mediated neuroprotection, functional blocking of G-CSFR was performed. Pretreatment of CGNs with anti G-CSFR antibody 30 minutes before glutamate treatment abolished G-CSF-mediated neuroprotection against glutamate-induced neuronal death (Fig. 2B).

Next, signaling pathways downstream of G-CSFR were blocked with specific inhibitors to clarify the contribution of each signaling pathway to the neuroprotective effects of G-CSF. Both the JAK2/STAT inhibitor AG490 and the PI3K inhibitor wortmannin partially abolished G-CSF-mediated neuroprotection against glutamate-induced neuronal death (Fig. 2C, D), whereas the mitogen-activated protein kinase inhibitor PD98059 had no influence on the neuroprotective effects of G-CSF.

Western blot analysis was performed to examine signaling events after G-CSF treatment. In cultured CGNs,

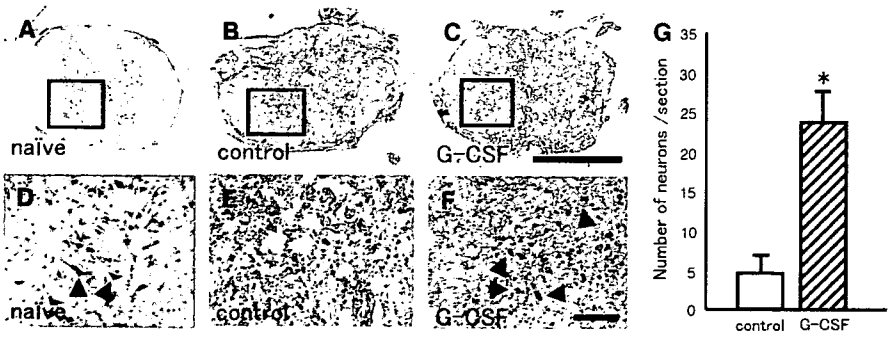

FIGURE 5. Histologic assessment with cresyl violet staining after spinal cord injury. Few neurons survived in the spinal cord of control mice 6 weeks after injury **(B, E)**. In the granulocyte colony-stimulating factor (G-CSF)-treated mice, increased neuronal survival was observed in the spinal cord 6 weeks after injury **(C, F**, arrowheads). Neurons in the anterior horn of the naive mouse spinal cords **(A, D**, arrowheads). Scale bars = **(A–C)** 1,000 μm; **(D–F)** = 100 μm. The number of surviving neurons in the G-CSF group was significantly larger than that of the control group **(G)**. The average number of the surviving neuron in the G-CSF group was 24.0/slice (hatched column), whereas neuronal survival in the control group was 4.6/slice (open column). Data are expressed as means ± SE. *, significant difference ($p < 0.05$).

the expression level of pSTAT3 increased by 15 minutes after G-CSF exposure, peaked 1 to 2 hours after exposure, and then decreased 6 hours after G-CSF treatment (Fig. 3). Levels of Bcl-2, an antiapoptotic target of STAT3, were elevated within 30 minutes of G-CSF exposure and remained elevated at 6 hours (Fig. 3). The expression level of total STAT 3 was unchanged during observation (Fig. 3). There was also no change in the expression level of actin, indicating equal protein loading (Fig. 3).

Immunohistochemical and Histologic Assessment

Our results using a model of compressive SCI demonstrate that G-CSF also exhibits neuroprotective effects in vivo. The number of cells double positive for Neu-N and cleaved caspase-3 was significantly smaller in the G-CSF-treated group than in the control group 1 day and 3 days after injury ($p < 0.05$) (Fig. 4). The average number of double positive cells for Neu-N and cleaved caspase-3 in the G-CSF group was 8.8 (5–13) 1 day after injury and 7.7 (3–11) 3 days after injury, whereas the number of apoptotic neurons in the control group was 16.3 (8–19) 1 day after injury and 14.1 (9–17) 3 days after injury, respectively.

Six weeks after injury, cresyl violet-positive neurons in the anterior horn of the spinal cord were counted as surviving neurons. The number of surviving neurons in the G-CSF group was significantly larger than that in the control group ($p < 0.05$) (Fig. 5). The average number of surviving neurons in the G-CSF group was 24.0/slice, whereas that in the control group was 4.6/slice.

Recovery of Hindlimb Motor Function

We assessed the recovery of hindlimb function using the motor function scale (10), in which the maximum hindlimb motor function scale score is 13. All mice had a score of 13 before surgery, and the score dropped to 0 immediately after the SCI. Significant recovery of hindlimb function was observed in mice from the G-CSF-treated group 4 weeks after injury compared with those of the vehicle-treated group ($p < 0.05$) (Fig. 6A). The average recovery score in the G-CSF group 6 weeks after injury was 4.0 (3–6), indicating stepping and forward propulsive movements of 1 hindlimb without weight bearing, whereas the average recovery score in the control group was 2.9 (2–5), indicating obvious movements of 1 or more joints in both hindlimbs without coordination, alternate stepping movements, or weight-bearing (Fig. 6B). The highest recovery score in the G-CSF group was 6, indicating weight-bearing ability of hindlimbs with abnormal walking (external rotation of 1 or both limbs and/or hip instability) whereas the highest recovery score in the control group was 5, indicating alternate stepping and forward propulsive movement of the hindlimbs without weight bearing.

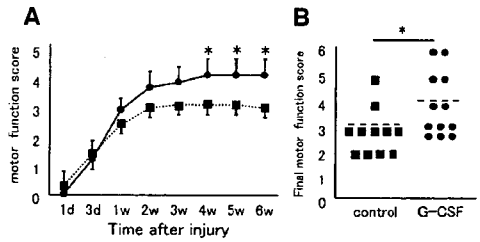

FIGURE 6. Hindlimb functional assessment using the motor functional scale (Farooque et al [10]). Time course of hindlimb functional recovery **(A)**, and comparison of final motor function score between the groups **(B)**. A significant recovery of hindlimb function was observed in granulocyte colony-stimulating factor (G-CSF)-treated mice (circles) 4 weeks after injury compared with the control group (**A**, squares) ($p < 0.05$). The average recovery score in the G-CSF-treated mice 6 weeks after injury was 4.0 (3–6) (**B**, circles), whereas the average recovery score in the control group was 2.9 (2–5) (**B**, squares). Data are expressed as means ± SE. *, significant difference ($p < 0.05$).

DISCUSSION

Our results from this study demonstrate that G-CSF prevented glutamate-induced neuronal death. Furthermore, administration of G-CSF prevented neuronal apoptosis during the acute phase after SCI, resulting in elevated neuronal survival in the spinal cord and improved hindlimb motor function 6 weeks after injury.

G-CSF regulates survival of postmitotic neutrophils by inhibition of apoptosis in the hematopoietic system with activation of the G-CSFR (11). Known signaling cascades downstream of G-CSFR are divided mainly into 2 classes, activation of the STAT family or the PI3K/Akt pathway. In hematopoietic lineage cells, G-CSF activates intracellular signaling pathways including STAT3 (12) and Akt (13), which are both linked to suppression of apoptosis and proliferation. The antiapoptotic function of STAT3 is mediated through its regulation of Bcl-2 expression (14). Akt promotes cell survival through multiple pathways, including the phosphorylation and inactivation of the proapoptotic protein BAD and through its induction of the antiapoptotic protein Bcl-2 (15–17). Recent reports have revealed that many basic cellular pathways are highly conserved between hematopoietic and neural cells. For instance, in addition to its expression in hemapoietic cells, G-CSFR is also expressed in neurons in the cerebral cortex (5), by Purkinje cells in the cerebellum and cerebellar nuclei (6), and by neurons and glial cells in the corpus callosum (5). G-CSF exerts antiapoptotic effects in these neurons through activation of pro-survival pathways similar to those in hemapoietic cells (18).

In the present study, we have confirmed that G-CSFR is expressed by cerebellar granule neurons in vitro and are the first to show that G-CSFR is also expressed by spinal cord neurons in vivo. Previous reports have shown that G-CSF treatment attenuates glutamate-induced neuronal death of CGNs (5), staurosporine-induced apoptosis of rat primary cortical neurons, and camptothecin-induced apoptosis of the human neuroblastoma cell line SHSY-5Y (6). Our results showed that simultaneous G-CSF administration had a partial neuroprotective effect against glutamate-induced neuronal death of CGNs. These results differ from those of Schäbitz et al (5), who reported that pretreatment with G-CSF completely suppressed glutamate-induced neuronal

death in CGNs. This discrepancy may be due to the difference in the time of G-CSF administration. Furthermore, we showed that pretreatment with anti-G-CSFR antibody completely abolished G-CSF-mediated neuroprotection against glutamate-induced neuronal death of CGNs, suggesting that G-CSF exerts its neuroprotective effect on CGNs via binding to G-CSFR. Schneider et al (6) have demonstrated that the antiapoptotic effects of G-CSF in rat primary cortical neurons treated with staurosporine and the human neuroblastoma cell line SHSY-5Y treated with camptothecin occurs via activation of PI3K/Akt pathway and could be abolished by the specific PI3K/Akt inhibitor LY294002. They also showed that activation of STAT3 and upregulation of its antiapoptotic target Bcl-xL were induced by G-CSF treatment in rat primary cortical neurons (6). Komine-Kobayashi et al (7) reported that G-CSF-induced activation of STAT3 and its antiapoptotic target Bcl-2 resulted in inhibition of apoptotic neuronal death after transient focal cerebral ischemia in mice. In the present study, G-CSF suppression of glutamate-induced cell death of cultured CGNs occurred via the activation of both the JAK/STAT and PI3K/Akt pathways, which could be abolished by their specific inhibitors. Moreover, the present results show that G-CSF promotes the activation of STAT3 and upregulation of Bcl-2 in cultured CGNs. These lines of evidence suggest that the neuroprotective effect of G-CSF is mediated at least partially via the activation of the JAK/STAT and PI3K/Akt pathways as previously reported (18).

Our in vivo results indicate that G-CSF suppressed neuronal apoptosis during the acute phase and increased the number of surviving neurons after the chronic phase of SCI, suggesting that G-CSF is also neuroprotective in vivo. In addition to its direct effects on spinal cord neurons, G-CSF has several actions in vivo that may contribute to neuroprotection. G-CSF suppresses inflammatory cytokines in experimental allergic encephalitis in mice (19) and tumor necrosis factor-α expression in lipopolysaccharide-stimulated human monocytes in vitro (20). Therefore, G-CSF may exert neuroprotective effects by suppressing inflammatory cytokine expression during the acute phase of SCI. G-CSF also can promote mobilization of bone marrow-derived cells and their migration into injured tissues including ischemic brain tissue (7, 21). Recently, Urdzikova et al (22) reported that subacutely (7–11 days postinjury) administered G-CSF promotes functional recovery after SCI in rats via mobilization of bone marrow cells.

Moreover, G-CSF has several actions on the vascular system, and, in a model of stroke, G-CSF suppresses brain edema formation (23) and promotes angiogenesis (24). Finally, G-CSF stimulates neurogenesis both directly (6) or via the upregulation of vascular endothelial growth factor (25). All of these mechanisms may contribute to the neuroprotective effects of G-CSF after SCI. Although this is the first report showing G-CSF-mediated neuroprotection that results in functional recovery, further exploration is needed to clarify the precise mechanism of action.

One of the major obstacles for conducting clinical trials for neuroprotective drugs is to first establish the safety and competency for use in human subjects. The complexity, size, and duration of clinical trials of novel drugs often make them quite costly to conduct and may impede the development of therapeutic agents that could have a significant impact in clinical practice. Therefore, although the efficacy of various drug therapies in models of SCI has been reported, few drugs have been practically carried into clinical trials. Thus, drugs with proven clinical exploitability have a significant advantage for clinical trials for novel therapeutic purposes. From this point of view, the currect use of G-CSF in the clinic for hematopoietic stimulation and its ongoing clinical trial for brain infarction (26) make it an appealing molecule that could be rapidly placed into trials for patients with acute SCI. Although many hurdles (e.g. optimal dosage, therapeutic time windows, and more precise mechanisms of action) still need to be resolved, the present results encourage us to pursue future clinical trials of G-CSF for patients with acute SCI.

ACKNOWLEDGMENT

The authors thank KIRIN Brewery (Tokyo, Japan) for kindly providing human recombinant G-CSF.

REFERENCES

1. Profyris C, Cheema SS, Zang DW, et al. Degenerative and regenerative mechanisms governing spinal cord injury. Neurobiol Dis 2004;15:415–36
2. Nicola NA, Metcalf D, Matsumoto M, et al. Purification of a factor inducing differentiation in murine myelomonocytic leukemia cells. Identification as granulocyte colony-stimulating factor. J Biol Chem 1983;258:9017–23
3. Roberts AW. G-CSF: A key regulator of neutrophil production, but that's not all! Growth Factors 2005;23:33–41
4. Harada M, Qin Y, Takano H, et al. G-CSF prevents cardiac remodeling after myocardial infarction by activating the Jak-Stat pathway in cardiomyocytes. Nat Med 2005;11:305–11
5. Schäbitz WR, Kollmar R, Schwaninger M, et al. Neuroprotective effect of granulocyte colony-stimulating factor after focal cerebral ischemia. Stroke 2003;34:745–51
6. Schneider A, Kruger C, Steigleder T, et al. The hematopoietic factor G-CSF is a neuronal ligand that counteracts programmed cell death and drives neurogenesis. J Clin Invest 2005;115:2083–98
7. Komine-Kobayashi M, Zhang N, Liu M, et al. Neuroprotective effect of recombinant human granulocyte colony-stimulating factor in transient focal ischemia of mice. J Cereb Blood Flow Metab 2006;26:402–13
8. Kamada T, Koda M, Dezawa M, et al. Transplantation of bone marrow stromal cell-derived Schwann cells promotes axonal regeneration and functional recovery after complete transection of adult rat spinal cord. J Neuropathol Exp Neurol 2005;64:37–45
9. Koda M, Hashimoto M, Murakami M, et al. Adenovirus vector-mediated in vivo gene transfer of brain-derived neurotrophic factor (BDNF) promotes rubrospinal axonal regeneration and functional recovery after complete transection of the adult rat spinal cord. J Neurotrauma 2004;21:329–37
10. Farooque M, Isaksson J, Olsson Y. Improved recovery after spinal cord injury in neuronal nitric oxide synthase-deficient mice but not in TNF-α-deficient mice. J Neurotrauma 2001;18:105–14
11. Hu B, Yasui K. Effects of colony-stimulating factors (CSFs) on neutrophil apoptosis: Possible roles at inflammation site. Int J Hematol 1997;66:179–88
12. Chakraborty A, White SM, Schaefer TS, et al. Granulocyte colony-stimulating factor activation of Stat3α and Stat3β in immature normal and leukemic human myeloid cells. Blood 1996;88:2442–49
13. Dong F, Larner AC. Activation of Akt kinase by granulocyte colony-stimulating factor (G-CSF): Evidence for the role of a tyrosine kinase activity distinct from the Janus kinases. Blood 2000;95:1656–62

14. Fukada T, Hibi M, Yamanaka Y, et al. Two signals are necessary for cell proliferation induced by a cytokine receptor gp130: Involvement of STAT3 in anti-apoptosis. Immunity 1996;5:449–60
15. Datta SR, Brunet A, Greenberg ME. Cellular survival: A play in three Akts. Genes Dev 1999;13:2905–27
16. del Peso L, Gonzalez-Garcia M, Page C, et al. Interleukin-3-induced phosphorylation of BAD through the protein kinase Akt. Science 1997; 278:687–99
17. Ahmed NN, Grimes HL, Bellacosa A, et al. Transduction of interleukin-2 antiapoptotic and proliferative signals via Akt protein kinase. Proc Natl Acad Sci U S A 1997;94:3627–32
18. Schneider A, Kuhn HG, Schäbitz WR. A role for G-CSF (granulocyte-colony stimulating factor) in the central nervous system. Cell Cycle 2005;4:1753–57
19. Zavala F, Abad S, Ezine S, et al. G-CSF therapy of ongoing experimental allergic encephalomyelitis via chemokine-and cytokine-based immune deviation. J Immunol 2002;168:2011–19
20. Nishiki S, Hato F, Kamata N, et al. Selective activation of STAT 3 in human monocytes stimulated by G-CSF: Implication in inhibition of LPS-induced TNF-α production. Am J Physiol Cell Physiol 2004;286: 1302–11
21. Kawada H, Takizawa S, Takanashi T, et al. Administration of hematopoietic cytokines in the subacute phase after cerebral infarction is effective for functional recovery facilitating proliferation of intrinsic neural stem/progenitor cells and transition of bone marrow-derived neuronal cells. Circulation 2006;113:701–10
22. Urdzikova L, Jendelova P, Glogarova K, et al. Transplantation of bone marrow stem cells as well as mobilization by granulocyte-colony stimulating factor promotes recovery after spinal cord injury in rats. J Neurotrauma 2006;23:1379–91
23. Gibson C, Jones C, Prior MLW, et al. G-CSF suppresses edema formation and reduces interleukin-1β expression after cerebral ischemia in mice. J Neuropathol Exp Neurol 2005;64:763–69
24. Lee ST, Chua K, Jung KH, et al. Granulocyte colony-stimulating factor enhances angiogenesis after focal cerebral ischemia. Brain Res 2005; 1058:120–28
25. Jung KH, Chu K, Lee ST, et al. Granulocyte colony-stimulating factor stimulates neurogenesis via vascular endothelial growth factor with STAT activation. Brain Res 2006;1073:190–201
26. Shyu WC, Lin SZ, Lee CC, et al. Granulocyte colony-stimulating factor for acute ischemic stroke: A randomized controlled trial. CMAJ 2006; 174:927–33

Available online at www.sciencedirect.com
ScienceDirect
Immunology Letters 114 (2007) 52–58
Immunology Letters
www.elsevier.com/locate/

Short communication

Erythroblasts highly express the ABC transporter Bcrp1/ABCG2 but do not show the side population (SP) phenotype

Kazumi Yamamoto, Shinya Suzu, Yuka Yoshidomi, Masateru Hiyoshi, Hideki Harada, Seiji Okada*

Division of Hematopoiesis, Center for AIDS Research, Kumamoto University, 2-2-1 Honjo, Kumamoto 860-0811, Japan

Received 5 December 2006; received in revised form 24 August 2007; accepted 26 August 2007
Available online 17 September 2007

Abstract

Stem cells in various somatic tissues including hematopoietic stem cells can be identified by the "side population (SP)" phenotype based on the efflux of Hoechst33342. Knockout and enforced expression experiments show that the expression of the Bcrp1/ABCG2 gene is an important determinant of the SP phenotype. In this study, we showed that erythroblasts also express a large amount of Bcrp1/ABCG2. The level of expression was increased with maturation, but did not relate to the cell-cycle status. Despite the high expression level of Bcrp1/ABCG2, erythroblasts did not show the "side population" phenotype. Furthermore, a Bcrp1/ABCG2 inhibitor, verapamil, had little effect on the Hoechst33342 staining pattern of erythroblasts. However protoporphyrin IX fluorescence was significantly higher in the presence of verapamil, suggesting that the ABCG2 functions as a transmembrane transporter in erythroblasts. These results indicate that dissociation between Bcrp1/ABCG2 expression and dye efflux function exists in erythroblasts and in stem cells, and that the function of ABCG2 in erythroblasts differs from that in stem cells.

Keywords: ABCG2; Erythroblast; Hoechst33342; Side population

1. Introduction

Hematopoietic stem cells can be identified by the "side population (SP)" phenotype, which is based on the efflux of the fluorescent dye Hoechst33342 and can be detected by flow cytometry [1,2]. SP cells have now been identified in many other tissue stem cells of various species as well as cancer stem cells [3,4]. Recently, it has become clear that an ABC transporter, ABCG2 (ATP-binding cassette, subfamily G, member 2), also known as breast cancer resistant protein (Bcrp-1) (Bcrp1/ABCG2), is mainly responsible for the SP phenotype [5–7]. However, ABCG2 is also detected in epithelial tissues such as the placenta, intestine, kidney and hepatic canalicular membrane [4,8]. As for the hematopoietic lineage, previous studies on mouse and human hematopoietic cells demonstrated that ABCG2 is highly expressed in primitive hematopoietic stem cells and is down-regulated in most committed progenitors, and sharply up-regulated during erythroid differentiation [5–7,9,10]. Although the exact physiologic roles of ABCG2 in these cells are not yet well known, it seems likely that an important function of ABCG2 is to protect against the cytotoxic actions of hypoxia or xenotoxins [4,6,7].

Here, we report that murine erythroblasts express a large amount of ABCG2; however, they do not show the "SP" phenotype by flowcytometry. Our data demonstrate a clear discrepancy between the expression of ABCG2 and "SP" phenotype and that the function of ABCG2 in erythroblasts differs from that in stem cells.

2. Materials and methods

2.1. Mice

C57/BL6 mice were purchased from Japan Clea. (Tokyo, Japan) and used in experiments between 8 and 12 weeks of age. All of the animal experiments were performed according to the guideline in the Institutional Animal Committee of Kumamoto University.

* Corresponding author. Tel.: +81 96 373 6522; fax: +81 96 373 6523.
E-mail address: okadas@gpo.kumamoto-u.ac.jp (S. Okada).

0165-2478/$ – see front matter © 2007 Elsevier B.V. All rights reserved.
doi:10.1016/j.imlet.2007.08.008

2.2. Monoclonal antibodies (mAbs)

FITC, PE, or APC-conjugated mAbs against Mac-1 (M1-70), TER119 (Ly-76), CD71 (C2), B220 (RA3-6B2), Gr-1 (RB6-8C5), CD34 (RAM34), CD4 (GK1.5) and CD8 (53-6.72) were purchased from BD Pharmingen (San Diego, CA) or eBioscience (San Diego, CA). APC-conjugated anti-Sca-1 (Ly6A/E) and PE-conjugated anti-c-kit (CD117) were purchased from BD Pharmingen and used to purify the primitive hematopoietic stem cell fraction [11].

2.3. Hoechst33342 staining

Bone marrow (BM) cells were flushed from their femurs with phosphate-buffered saline (PBS) supplemented with 3% fetal calf serum (FCS). The suspension was washed and passed through a 70-μm nylon filter to produce a single-cell suspension. Mature red blood cells were lysed with ACK lysing buffer (0.155 M ammonium chloride, 0.1 M disodium EDTA, and 0.01 M potassium bicarbonate). The BM cells were resuspended at 1×10^6 cells/ml in 3% FCS/RPMI1640 medium with 5 μg/ml Hoechst33342 (Molecular Probe, Eugene, OR) for 60 min at 37 °C. For the inhibitor experiments, 50 μM verapamil (Sigma) was added to cells, and cells were incubated for 15 min at 37 °C, then Hoechst33342 was added [1,2]. The Hoechst-stained cells were resuspended in ice-cold staining medium (PBS with 3% FCS and 0.1% sodium azide) and stained for 30 min on ice with mAbs. Cells were washed and resuspended in staining medium supplemented with 1 μg/ml propidium iodide (PI) for flow cytometric analysis and cell sorting.

2.4. Flow cytometric analysis and cell sorting

Analysis and cell sorting were performed on a triple-laser JSAN flow cytometer (Bay Bioscience, Kobe, Japan) equipped with a 375 nm UV diode laser, 488 nm blue diode laser, and 633 nm red diode laser. The Hoechst33342 dye was excited with 375 nm ultraviolet light and the resultant fluorescence was measured at two wavelengths using 422/44 nm BP and 590/35 nm BP filters for the detection of Hoechst blue and red, respectively. A 530 nm long pass dichroic mirror (DCLP) was used to separate the emission wavelengths. Analysis was also performed on a LSR II flow cytometer (Becton Dickinson, Mountain View, CA) equipped with a 350 nm UV diode laser, 408 nm violet diode laser, 488 nm blue diode laser, and 633 nm red diode laser. Multiparameter data were analyzed using the FlowJo program (Tree Star, Ashland, OR).

2.5. RT-PCR analysis

Total RNA was extracted from sorted BM cells using a Trizol Reagent (Gibco BRL, Grand Island, NY). RNAs were reverse-transcribed using Superscript II (Life Technologies, Grand island, NY) and oligo(dT) (Pharmacia, Piscataway, NJ) in a final volume of 20 μl. A Semiquantitative RT-PCR of the ABCG2 transcript in sorted cell populations was performed by amplification of the GAPDH-normalized RT reactions. After an initial 7 min of incubation at 95 °C, 30 cycles of PCR were carried out under the following conditions: denaturation at 95 °C for 60 s, annealing at 60 °C for 40 s, and polymerization at 72 °C for 60 s. Primers for the cDNA amplification were as follows: ABCG2 primers, 5′-CCATAGCCACAGGCCAAAGT-3′ and 5′-GGGCCACATGATTCTTCCAC-3′; G3PDH primers, 5′-TGAAGGTCGGTGTGAACGGATTTGGC-3′ and 5′-CATGTAGGCCATGAGGTCCACCAC-3′. The PCR products were separated on a 1.2 % agarose gel and stained with ethidium bromide.

2.6. Real time PCR

Real time PCR was performed on a Thermal Cycler Dice Real Time System (Takara Bio., Japan) using a SYBERExScript RT-PCR kit (Takara Bio.) according to manufacturer's instruction. The primers used for real time PCR were designed by Takara Bio: ABCG2, MA030903; GAPDH, MA023937.

2.7. Western blot analysis

Total proteins from sorted cells were extracted with RIPA buffer. Lysates were clarified by centrifugation. Samples were electrophoresed through 7.5% SDA-PAGE gels and transferred to a nylon membrane (Hybond-P, GE Healthcare Bio-Science, NJ). After blocking with Block Ace (Dainippon Sumitomo Pharma, Japan), the membrane was reacted with a 1/100 dilution of anti-ABCG2 antibody (BXP-53) (Monosan, The Netherlands) for 1 h at room temperature. Detection was performed using the enhanced chemiluminescence Western Blotting detection system (ECL, GE Healthcare Bio-Science) with HPR-conjugated Goat anti-rat immunoglobulins (Dako).

2.8. Cellular protoporphyrin IX (PPIX) measurements

Cellular PPIX concentration was measured as described previously [10]. For PPIX efflux assays, cells were incubated with 10 μM PPIX (Sigma) in 10% FCS/DMEM for 30 min at 37 °C, washed once with medium, and incubated at 37 °C for 1 h. Verapamil (50 μM), if used, was present during the entire procedure. Cells were spun down, resuspended into staining medium, and analyzed in a flow cytometry (LSR II) for PPIX fluorescence using a 695/40-nm filter after excitation by a 408 nm Violet light. For endogenous PPIX assays, BM cells were treated with 1mM δ-aminolevulinic acid (ALA) (Sigma) for 21 h, washed once with PBS, stained with TER119-APC and CD71-FITC, and directly analyzed in a LSR II flow cytometry for PPIX fluorescence.

3. Results and discussion

3.1. Erythroblasts express high levels of ABCG2 mRNA and protein

Although ABCG2 is responsible for the SP phenotype, it is known to be expressed in cells other than stem cells [4,5]. As for the hematopoietic lineage, hematopoietic stem cells, erythrob-

lasts, and NK cells express ABCG2 [5,10,12]. To determine the level of expression of ABCG2 in bone marrow cells, a subpopulation of bone marrow and spleen cells was isolated by flow cytometric sorting. RT-PCR analysis showed that ABCG2 mRNA was present in the erythroid lineage (TER119$^+$ cells) but little expressed in the myeloid, B lymphoid and T lymphoid lineages (Fig. 1A). Western blot analysis showed that ABCG2 protein was present only in erythroblasts (Fig. 1B).

Erythroblasts can be divided into four subsets (R1: TER119^{low}CD71^{high}, R2: TER119^{high} CD71^{high}, R3: TER119^{high}CD71^{med}, R4: TER119^{high}CD71$^{low\text{-}negative}$) based on simultaneous immunostaining with anti-TER119 and anti-CD71 mAbs (Fig. 1C) [13,14]. Erythroblasts sequentially differentiate from proerythroblasts (R1) into basophilic erythroblasts (R2), polychromatophilic erythroblasts (R3), and orthochromatophilic erythroblasts and reticulocytes (R4) [14]. Semiquantative RT-PCR revealed that the level of expression of ABCG2 mRNA was higher at all stages in erythroblasts than in the hematopoietic stem cell fraction (KSL cells) (Fig. 1D). This explains why less than 10% of KSL cells are CD34$^-$ primitive hematopoietic stem cells highly expressing ABCG2 and with the differentiation into CD34$^+$KSL cells, they lose ABCG2 expression rapidly [5]. To further assess the expression of ABCG2 mRNA, real time RT-PCR was performed. As shown in Fig. 1E, the ABCG2 mRNA level increased with the erythroid maturation. Our data obtained with fresh erythroblasts were consistent with the results of Zhou et al. [5,10], who showed that ABCG2 mRNA expression is up-regulated with erythroid maturation using erythroid cell lines, MEL and K562, and cultured erythroblasts. It is interesting note that the expression of ABCG2 mRNA was high in erythroblasts as in CD34$^-$KSL cells. These data are in consistent with the ABCG2 knock in mouse study, in which GFP expression was observed only in TER119 positive cells and hematopoietic stem cells [15].

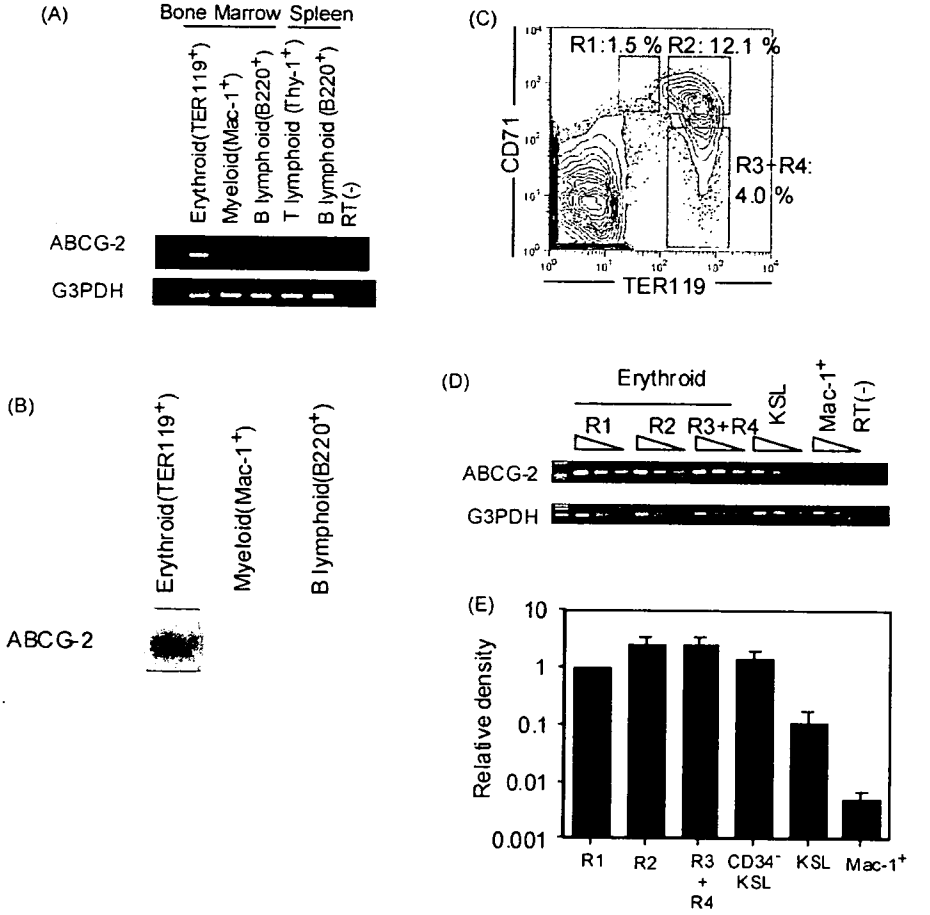

Fig. 1. Expression of ABCG2 in the erythroblast subsets. (A) ABCG2 mRNA expression was analyzed in erythroid cells (TER119$^+$), myeloid cells (Mac-1$^+$), B lymphoid cells (B220$^+$) and T lymphoid cells (Thy-1$^+$) isolated from BM or spleen. (B) Western blot analysis of the ABCG2 protein in erythroid cells (TER119$^+$), myeloid cells (Mac-1$^+$) and B lymphoid cells (B220$^+$) isolated from BM. (C) The BM cells were stained with anti-TER119 and anti-CD71 mAbs and analyzed using a JSAN flow cytometer. Erythroblasts sequentially differentiate from R1 (TER119^{low}CD71^{high}) into R2 (TER119^{high}CD71^{high}) cells, R3 (TER119^{high}CD71^{med}) cells, and R4 (TER119^{high}CD71$^{low\text{-}negative}$) cells. (D) ABCG-2 expression was analyzed by semiquantitative RT-PCR in immature to mature erythroblasts (R1–R4), the hematopoeitic stem cell fraction (Lin$^-$c-kit$^+$Sca-1$^+$) and myeloid (Mac-1$^+$) cells. cDNAs serially diluted eight times were used for PCR. Results are representative of three independent experiments. (E) ABCG2 expression was analyzed by real-time PCR in immature to mature erythroblasts (R1–R4), the hematopoietic stem cell fraction (Lin$^-$c-kit$^+$Sca-1$^+$) and myeloid (Mac-1$^+$) cells. The copy numbers of ABCG2 mRNA were quantified by comparison with a standard curve. Values were normalized to mouse G3PDH expression, which was used as the endogenous control.

3.2. Erythroblasts do not show the SP phenotype in spite of high expression of ABCG2

To further analyze the relationship between ABCG2 expression and the SP phenotype, we stained the bone marrow cells with Hoechst33342, Sca-1-FITC, c-kit-APC, and TER119-PE, simultaneously, analyzed them using flow cytometry, and drew up plots of Hoechst33342 red/blue fluorescence. Whole BM cells had the SP phenotype as previously described [1], and most cells with the SP phenotype were positive for Sca-1 and c-kit (Fig. 2A), but negative for Mac-1, B220, and TER119 (data not shown). In contrast, TER119$^+$ cells did not have the SP phenotype (Fig. 2B). These results clearly demonstrate the dissociation between ABCG2 expression and the dye-efflux function of ABCG2. As Hoechst33342 can be excited with a UV laser and is a cell membrane-permeant DNA-selective binding dye, it was originally used in cell-cycle studies [16]. TER119$^+$ cells were divided into three fractions based on the pattern of staining by Hoechst blue (Fig. 2B), i.e. subdiploid (G1), G0/G1 phase (G2) and S/G2/M phase (G3). We compared the expression levels of ABCG2 by semiquantitative RT-PCR. As shown in Fig. 2C, ABCG2 mRNA expression was not linked to the cell-cycle state of erythroblasts.

ABCG2 has been identified as responsible for the SP phenotype [5]. In fact, overexpression of ABCG2 increased the SP phenotype [5], and mice deficient in ABCG2 lacked the side population in bone marrow [6]. Since then, the SP phenotype has been used as a stem cell marker and to isolate the stem cell fraction. However, Morita et al. recently demonstrated the existence of a non-SP ABCG2-expressing hematopoietic stem cell fraction [17]. Their data imply a dissociation between ABCG2 expression and the dye-efflux function of Bcrp1/ABCG2.

3.3. Effects of an ABCG2 inhibitor, verapamil, on Hoechst33342 staining pattern and protoporphyrin IX efflux of erythroid lineage

The SP phenotype is caused by the active efflux of Hoechst33342 via ABCG2 [5], and this mechanism can be inhibited by ABC transporter inhibitors [1,2]. To determine whether ABCG2 activity was involved in the phenotype of the erythroid lineage, the effect of verapamil, an ABCG2

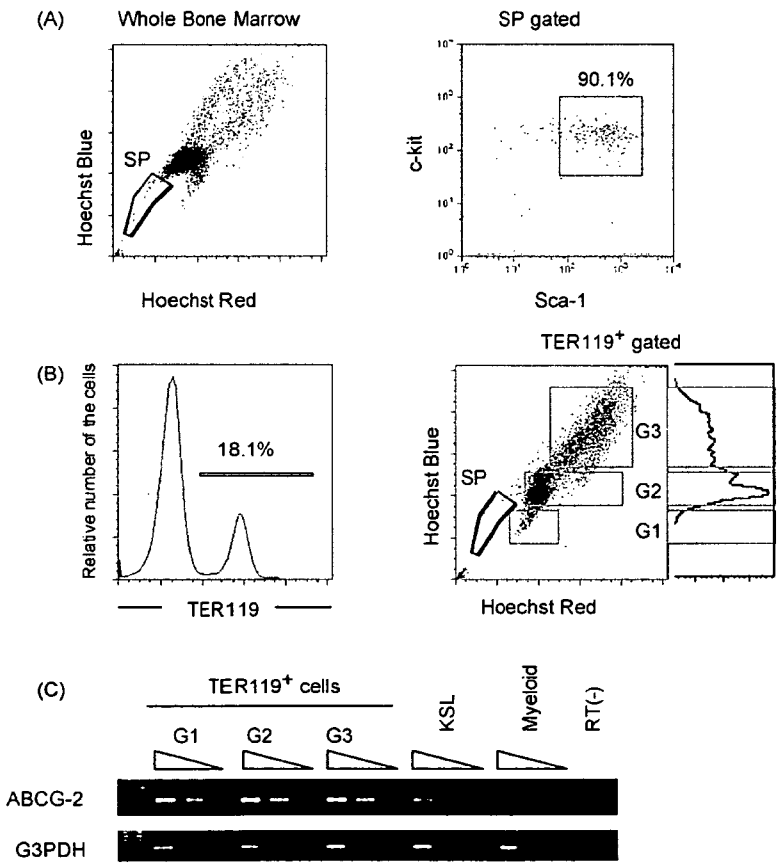

Fig. 2. Erythroblasts do not show the SP phenotype but highly express ABCG2 mRNA. Whole BM cells were stained with Hoechst33342, followed by c-kit-FITC, Sca-1-APC and TER119-PE, and analyzed on a flow cytometry. (A) A display of whole BM cells on a Hoechst red/blue plot reveals the side population. In contrast, TER119$^+$ cells contained very few SP cells. (B) TER119$^+$ cells are divided into three fractions based on the pattern of staining by Hoechst blue, i.e.: subdiploid (G1), G0/G1 phase (G2), and S/G2/M phase (G3). (C) The expression of ABCG2 was examined by RT-PCR. cDNA was synthesized from total RNA extracted from the three sorted erythroid fractions (G1, G2, and G3), the hematopoietic stem cell fraction (Lin$^-$c-kit$^+$Sca-1$^+$), and myeloid (Mac-1$^+$) cells. cDNAs serially diluted eight times were used for PCR. Results are representative of three independent experiments.

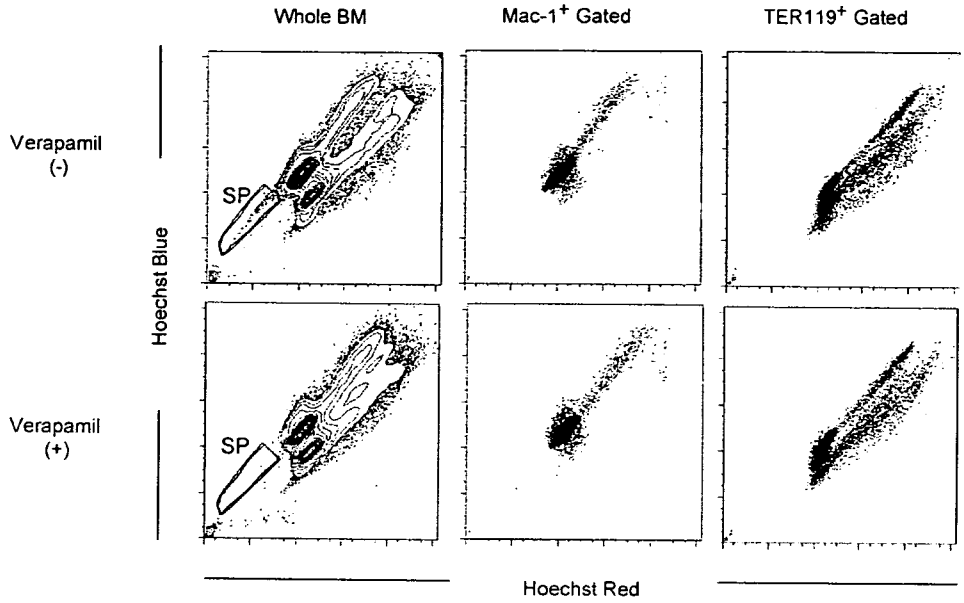

Fig. 3. Influence of verapamil (an ABCG2 inhibitor) on the Hoechst red/blue profile of whole BM, myeloid (Mac-1$^+$), and erythroid (TER119$^+$) cells. Whole BM cells were stained with Hoechst33342 in the presence or absence of verapamil, followed by Mac-1-FITC and TER119-PE, and analyzed on a flow cytometry. A display of whole BM cells on a Hoechst red/blue plot reveals the side population (SP). The SP fraction (R1) disappeared in the presence of verapamil, but it had no influence on the Hoechst red/blue profile of myeloid (Mac-1$^+$) and erythroid (TER119$^+$) cells.

inhibitor, was assessed. The SP fraction was markedly reduced in the presence of this ABC transporter inhibitor (50 μg/ml), as expected (Fig. 3). On the other hand, verapamil did not affect the Hoechst33342 staining patterns of both ABCG2 negative myeloid (Mac-1$^+$) and ABCG2 positive erythroid (TER119$^+$) cells, suggesting that although ABCG2 is highly expressed in erythroid cells, it dose not work for effective pump in erythroblasts. In order to determine if endogenously expressed ABCG2 in erythroid cells work effectively or not, we analyzed the effect of verapamil for efflux of exogenous protoporphirin IX (PPIX), as PPIX is the direct and natural substrate for ABCG2 [10]. Murine BM cells were incubated with PPIX with or without verapamil, and PPIX fluorescence was determined by flow cytometry. The PPIX fluorescence was significantly higher in the presence of verapamil (Fig. 4), showing that ABCG2 functions as effective transporter in primary erythroblasts. Although the PPIX fluorescence level differed, the PPIX fluorescence was significantly higher in the presence of verapamil in all of the erythroid subfractions. This result was confirmed with another experiment (Fig. 4) in which BM cells were treated with δ-ALA, which produce endogenous PPIX in erythroid cells. These results indicate that although ABCG2 is functionally expressed in erythroid cells, the function of ABCG2 in erythroblasts differs from that in stem cells. Such speculation is supported by reports that hematopoietic stem cells are relatively resistant to anticancer reagents such as 5-FU compared to the erythroid lineage [18,19]. In addition, Zong et al. demonstrated that the expression of ABCG2 during hematopoiesis is transcriptionally regulated by the alternative use of multiple leader exons and promoters in a developmental stage-specific manner [20]. In their observation, the expression patterns of ABCG2 mRNA isoforms were different between murine hematopoietic stem cells and erythroid cells.

ABCG2-deficient mice developed by Jonker et al. appeared normal, and hematocrit and hemoglobin levels were compatible between the wild-type and ABCG2-deficient mice [21], suggesting normal activity of heme synthesis-related enzymes under steady state conditions. Recently, Krishnamurthy et al. showed that ABCG2 specifically bound heme, and enhanced hypoxic cell survival [22]. They also demonstrated that ABCG2 expression was up-regulated by hypoxia, which involved the hypoxia-inducible transcription factor complex HIF-1. These mechanisms are largely responsible for the survival of hematopoietic stem cells in the hypoxic osteoblastic niche [23,24]. But it is unclear whether this mechanism works in erythroblasts or not. Also, it is unknown why ABCG2 does not function in the efflux of Hoechst33342 dye in erythroblasts. One possible explanation is that since erythroblasts contain a large amount of heme, most of the ABCG2 binds with heme [22] and heme bound ABCG2 may not function as a transmembrane transporter. This is supported by the fact that the expression of ABCG2 is up-regulated with erythroid differentiation, since the synthesis of heme also increases with erythroid differentiation [25,26]. Another explanation is that although ABCG2 expression is essential for Hoechst dye efflux, additional gene is needed to exhibit the "side population" which lack in erythroblasts. This is supported by the fact that erythroid cells and hematopoietic stem cells use different promoters to control the initiation of ABCG2 transcription [20], and therefore it is controlled by different mechanisms.

In summary, we showed that freshly isolated murine erythroblasts highly expressed functional ABCG2 but did not exhibit the "side population" phenotype, suggesting that ABCG2 is necessary but not sufficient for the exhibition of "side population". Further investigation of the functional role of ABCG2

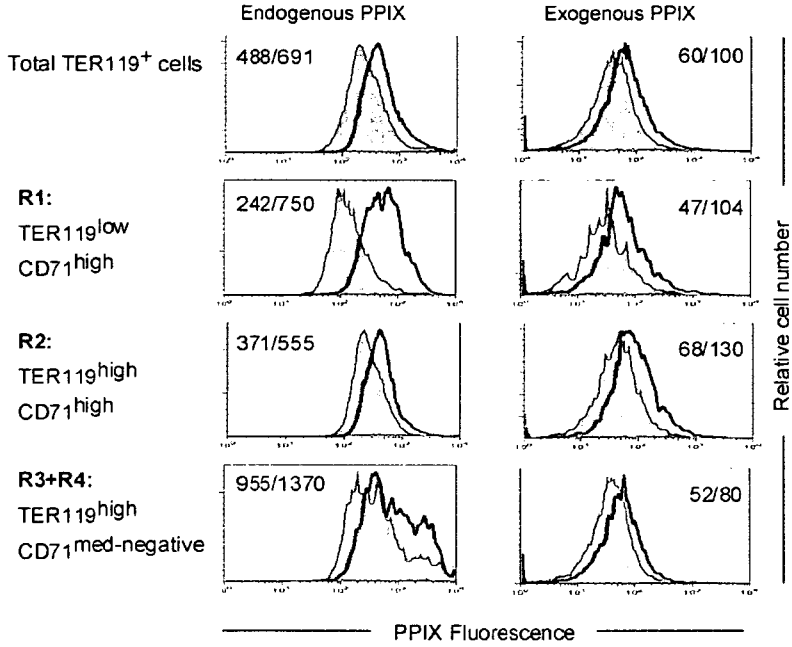

Fig. 4. Influence of verapamil on the endogenous and exogenous efflux of PPIX from erythroblasts. BM cells were incubated with (A) δ-ALA or (B) PPIX, with verapamil (solid line) or without verapamil (shaded area) and analyzed for PPIX fluorescence of erythroblast subfraction. The numbers in the graph show the mean fluorescence intensity (MFI) of PPIX fluorescence without/with verapamil. In all erythroblasts subfraction, PPIX fluorescence was significantly increased by treatment with verapamil.

signaling and its molecular mechanisms, especially differences between stem cells and erythroblasts, will provide a clue as to how stem cells are maintained and regulated by membrane transporters.

Acknowledgments

We are grateful to Ms. Y Endo for secretarial assistance, and Ms. I. Suzu for skillful technical assistance. This work was supported in part by Health and Labour Sciences Research Grants from the Ministry of Health, Labour and Welfare of Japan and by grants from the Ministry of Education, Science, Sports, and Culture of Japan.

References

[1] Goodell MA, Brose K, Paradis G, Conner AS, Mulligan RC. Isolation and functional properties of murine hematopoietic stem cells that are replicating in vivo. J Exp Med 1996;183:1797–806.
[2] Goodell MA, Rosenzweig M, Kim H, Marks DF, Demaria M, Paradis G, et al. Dye efflux studies suggest that hematopoietic stem cells expressing low or undetectable levels of CD34 antigen exist in multiple species. Nat Med 1997;3:1337–45.
[3] Challen GA, Little MH. A side order of stem cells: the SP phenotype. Stem Cells 2006;24:3–12.
[4] Doyle LA, Ross DD. Multidrug resistance mediated by the breast cancer resistant protein BCRP (ABCG2). Oncogene 2003;22:7340–58.
[5] Zhou S, Schuetz JD, Bunting KD, Colapietro AM, Sampath J, Morris JJ, et al. The ABC transporter Bcrp1/ABCG2 is expressed in a wide variety of stem cells and is a molecular determinant of the side-population phenotype. Nat Med 2001;7:1028–34.
[6] Zhou S, Morris JJ, Barnes Y, Lan L, Schuetz JD, Sorrentino BP. Bcrp1 gene expression is required for normal numbers of side population stem cells in mice, and confers relative protection to mitoxantrone in hematopoietic cells in vivo. Proc Natl Acad Sci USA 2002;99:12339–44.
[7] Scharenberg CW, Harkey MA, Torok-Storb B. The ABCG2 transporter is an efficient Hoechst 33342 efflux pump and is preferentially expressed by immature human hematopoietic progenitors. Blood 2002;99:507–12.
[8] Staud F, Pavek P. Breast cancer resistance protein (BCRP/ABCG2). Int J Biochem Cell Biol 2005;37:720–5.
[9] Tadjali M, Zhou S, Rehg J, Sorrentino BP. Prospective isolation of murine hematopoietic stem cells by expression of an Abcg2/GFP allele. Stem Cells 2006;24:1556–63.
[10] Zhou S, Zong Y, Ney PA, Nair G, Stewart CF, Sorrentino BP. Increased expression of the Abcg2 transporter during erythroid maturation plays a role in decreasing cellular protoporphyrin IX levels. Blood 2005;105:2571–6.
[11] Okada S, Nakauchi H, Nagayoshi K, Nishikawa S, Miura Y, Suda T. In vivo and in vitro stem cell function of c-kit- and Sca-1-positive murine hematopoietic cells. Blood 1992;80:3044–50.
[12] Pearce DJ, Ridler CM, Simpson C, Bonnet D. Multiparameter analysis of murine bone marrow side population cells. Blood 2004;103:2541–6.
[13] Socolovsky M, Nam H, Fleming MD, Haase VH, Brugnara C, Lodish HF. Ineffective erythropoiesis in Stat5a$^{-/-}$5b$^{-/-}$ mice due to decreased survival of early erythroblasts. Blood 2001;98:3261–73.
[14] Asari S, Sakamoto A, Okada S, Ohkubo Y, Arima M, Hatano M, et al. Abnormal erythroid differentiation in neonatal bcl-6-deficient mice. Exp Hematol 2005;33:26–34.
[15] Tadjali M, Zhou S, Rehg J, Sorrentino BP. Prospective isolation of murine hematopoietic stem cells by expression of an Abcg2/GFP allele. Stem Cells 2006;24:1556–63.
[16] Shapiro HM. Flow cytometry of DNA content and other indicators of proliferative activity. Arch Pathol Lab Med 1989;113:591–7.
[17] Morita Y, Ema H, Yamazaki S, Nakauchi H. Non-side-population hematopoietic stem cells in mouse bone marrow. Blood 2006;108:2850–6.
[18] Zant GV. Studies of hematopoietic stem cells spared by 5-fluorouracil. J Exp Med 1984;159:679–90.
[19] Weiterova L, Hofer M, Pospisil M, Znojil V, Vacha J, Vacek A, et al. Influence of the joint treatment with granulocyte colony-stimulating fac-